

A-CD Estrogens. I. Substituent Effects, Hormone Potency, and Receptor Subtype Selectivity in a New Family of Flexible Estrogenic Compounds

James S. Wright,^{*,†} Hooman Shadnia,[†] James M. Anderson,[†] Tony Durst,^{*,‡} Muhammad Asim,[‡] Mohamed El-Salfiti,[‡] Christine Choueiri,[‡] M. A. Christine Pratt,[§] Samantha C. Ruddy,[§] Rosanna Lau,[§] Kathryn E. Carlson,^{||} John A. Katzenellenbogen,^{||} Peter J. O'Brien,[⊥] and Luke Wan[⊥]

[†]Department of Chemistry, Carleton University, 1125 Colonel By Drive, Ottawa, Ontario, K1S 5B6, Canada,

[‡]Department of Chemistry, University of Ottawa, D'Iorio Hall, 10 Marie Curie Street, Ottawa, Ontario, K1N 6N5, Canada,

[§]Department of Cellular and Molecular Medicine, Faculty of Medicine, University of Ottawa, 451 Smyth Road, Ottawa, Ontario, K1H 8M5, Canada, ^{||}Department of Chemistry, University of Illinois, Urbana, Illinois 61801, United States, and [⊥]Faculty of Pharmacy, University of Toronto, 144 College Street, Toronto, Ontario, M5S 3M2, Canada

Received April 27, 2010

Long-term use of estrogen supplements by women leads to an increased risk of breast and uterine cancers. Possible mechanisms include metabolism of estradiol and compounds related to tumor-initiating quinones, and ligand-induced activation of the estrogen receptors ER α and ER β which can cause cancer cell proliferation, depending on the ratio of receptors present. One therapeutic goal would be to create a spectrum of compounds of variable potency for ER α and ER β , which are resistant to quinone formation, and to determine an optimum point in this spectrum. We describe the synthesis, modeling, binding affinities, hormone potency, and a measure of quinone formation for a new family of A-CD estrogens, where the A–C bond is formed by ring coupling. Some substituents on the A-ring increase hormone potency, and one compound is much less quinone-forming than estradiol. These compounds span a wide range of receptor subtype selectivities and may be useful in hormone replacement therapy.

Introduction

The safety of long-term steroid usage by women for purposes of hormone replacement therapy (HRT^o) or oral contraception (OC) is currently under scrutiny. On the basis of epidemiological evidence showing an increased risk of breast and uterine cancers associated with HRT usage,^{1–6} current medical thinking suggests that women should minimize their usage of hormone supplements. New evidence for the increased risk is the dramatic drop in breast cancer rates as of 2003, which has been attributed to the decline in use of HRT.⁷ However, the very widespread use of hormone supplements prior to 2003 is a testament to their efficacy in blocking symptoms associated with menopause. Preferably, a safer, noncarcinogenic compound will become available as an alternative to traditional steroids used as hormone supplements.

The etiology of breast cancer is complex, with hormone-dependent and hormone-independent components. It was originally thought that the only relation between estrogens and cancer was through their ability to stimulate abnormal cell proliferation via estrogen-receptor mediated processes. However, as

a result of new evidence on the relationship between estrogens and cancer, the field is undergoing a “paradigm shift”. A new mechanism of interest, which involves the formation of catechol estrogens as metabolites and their subsequent oxidation to carcinogenic quinones, is not yet considered proven to be the dominant cause of breast cancer, but an increasing amount of evidence in its favor is appearing.^{8–18}

We have encountered this oxidative reaction mechanism in our work on catecholic antioxidants.^{19–22} More importantly, in the course of this work we redesigned antioxidants to avoid the formation of cytotoxic quinones, a development that is also relevant to HRT. For example, consider the naturally occurring human estrogens estradiol and estrone, which have the classic steroid structure containing the A, B, C, and D rings, shown in Figure 1. The B, C, and D rings are saturated, but the A-ring is an aromatic phenol. Phenols are easily metabolized in the liver and elsewhere by cytochrome P450 hydroxylase.²³ This leads to hydroxyl substitution at the positions ortho to the aromatic hydroxyl group (i.e., positions 2 and 4 in the A-ring, using steroid notation), forming 2-OH estradiol and 4-OH estradiol. These metabolites, termed the “catechol estrogens”,⁹ can be further metabolized by oxidizing substances present in the cell, e.g., peroxidase/P450 or tyrosinase/O₂,²⁴ or even simply in the presence of oxygen (autooxidation) to give the corresponding 2,3-quinone and the 3,4-quinone.^{8–18}

Quinones in general have a tendency to be tumor initiators and/or promoters, and several such mechanisms are known.²³ They can damage DNA by combining with nucleic acid bases, thus causing replication errors. They can deplete essential cellular antioxidants such as glutathione and thiol-containing

*To whom correspondence should be addressed. For J.S.W. (nonsynthetic aspects): phone, (613) 520-2600, extension 3645; fax, (613) 520-3749; e-mail, jim_wright@carleton.ca. For T.D. (synthesis): phone, (613) 562-5800, extension 6072; fax, (613) 562-5170; e-mail, tony.durst@uottawa.ca.

^a Abbreviations: RBA, relative binding affinity; RTA, relative transcription activation; HRT, hormone replacement therapy; OC, oral contraception; ER α , estrogen receptor α ; ER β , estrogen receptor β ; E2, 17 β -estradiol; E1, estrone; CEE, conjugated equine estrogens; LBD, ligand binding domain; ERE, estrogen response element; BDE, bond dissociation enthalpy; MMFF, Merck molecular force field; DFT, density functional theory.

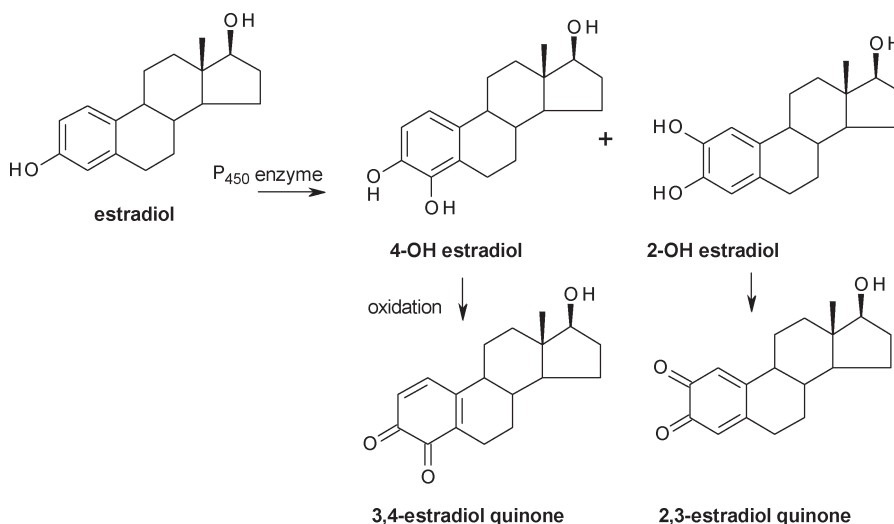


Figure 1. Hydroxylation of estradiol to form the catechol estrogens 2-OH estradiol and 4-OH estradiol, followed by their oxidation to form the corresponding 2,3- and 3,4-quinones.

proteins, subjecting the cell to oxidative stress. They can act directly as free radical generators via reduction to the semiquinone form and subsequent redox cycling, producing superoxide ion. Different quinones show differing degrees of cytotoxicity because of these competing mechanisms; e.g., some members of the family of naphthoquinones and anthraquinones are highly cytotoxic.²⁵

In Figure 1, starting from the natural hormone 17β-estradiol (hereafter “estradiol” or **E2**), the quinone formed involves only the A-ring; i.e. it is a benzoquinone. In the case of one of the conjugated equine estrogens (CEEs) also present in the HRT drug Premarin, the naphthoquinone was formed and it was found that hamsters treated with the naphthoquinone for 9 months showed 100% tumor incidence.^{11,12} This led Liehr, Cavalieri, Bolton, and co-workers to the conclusion that *quinone formation is causally related to the carcinogenic process*.^{8,12,15–17} The purpose of this paper is to design, synthesize, and test new molecules that structurally strongly resemble **E2** and retain hormonal potency while incorporating features that will retard or prevent quinone toxicity. As the title suggests, our focus will be on synthetic structures closely related to estradiol but where part of the steroid B-ring has been omitted. We also consider the selectivity of A-CD ligands for the two estrogen receptors ERα and ERβ, since it is hypothesized that selectivity for ERβ can be a desirable therapeutic feature.^{26–28}

The basic requirements for an estrogen receptor-active pharmacophore (either ERα or ERβ) have been summarized previously by one of the present authors.^{29,30} By use of steroid notation, there are two H-bonding “anchors” located near the 3-position (phenolic OH) and the 17-position (17β-OH in **E2**). H-bonding at the 3-position also involves a water molecule which forms a bridge between glutamate and arginine residues in the receptor and the phenolic OH group. The total free energy of binding of **E2** to either receptor is ~12 kcal/mol, leading to subnanomolar dissociation constants ($K_d = 0.2$ nM for **E2** in ERα and 0.5 nM in ERβ).^{29,30} Measurements using isothermal titration calorimetry³¹ have shown that at room temperature about 2 kcal/mol of this binding is due to the 3-OH and 0.5 kcal/mol to the 17-OH group. An additional ~3 kcal/mol of binding comes from a hydrophobic scaffold connecting the H-bond anchors. There is one important water molecule present in the active site of the crystal structure (for example, 1GWR.pdb for ERα and 1X7R.pdb for ERβ) which was

retained in the docking. In **E2** the O–O interatomic distance is 11.0 Å, and in general it is thought that for optimum hydrogen bonding this distance should be 11.0 ± 0.5 Å.^{32–35}

Selectivity of a ligand for the receptors ERα or ERβ depends on a number of factors, including the size and shape of the ligand-binding domain (LBD) and the specific interactions with the residues surrounding it.^{32,36–40} The active site cavity of ERβ is known to be smaller than that of ERα.^{29,32} Using a grid-based algorithm (see Docking and Scoring near end of Experimental Section), we determined the active site volumes to be 379 Å³ for ERα and 279 Å³ for ERβ. For comparison, ligand volumes are 282 Å³ for **E2** and only 259 Å³ for our compound **1a**. This suggests that the fit for **E2** in ERβ is tight, which results in the lower binding affinity of **E2** for this subtype. As will be seen, an increase in molecular volume beyond that of **1a** leads to a decrease in selectivity.

A communication on A-CD estrogens by the present authors described their synthesis and reported that some of these compounds showed strong hormonal potency coupled with good receptor selectivity.⁴¹ There have been several reports in the literature of A-CD compounds showing estrogenic activity prior to our own communication; these compounds have also been termed “B-ring seco-steroids” and ring B seco-estradiols”. To the best of our knowledge, the first such structures were reported in 1959 by Novello who termed the A-CD structures hexahydroindanes.⁴² Bindra, Neyyarapally, and co-workers^{43,44} studied estrogenic activity in A-CD compounds and in related compounds where the chirality is inverted at C9. They showed estrogenic and antifertility activity in rats for such compounds, although at doses that were 2 orders of magnitude greater than those required to show a similar response (e.g., uterine weight gain) from the natural hormone estrone. Agoston and co-workers^{45–48} have reported studies on many seco-steroids and discussed their use as antifertility and antiproliferative agents. Several comprehensive studies of structure–activity relationships for natural, synthetic, and environmental estrogens included many structures, where one of the steroid rings had been omitted, and considered the bonding requirements for an ideal pharmacophore.^{49,50} One of the present authors and his co-worker (J.A.K.) has also examined several seco-estrogens containing three rings and considered the factors that lead to differences in receptor-subtype selectivity.^{51,52}

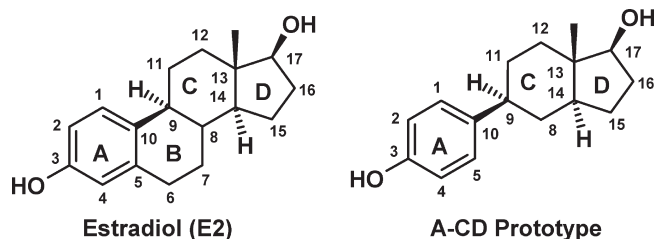
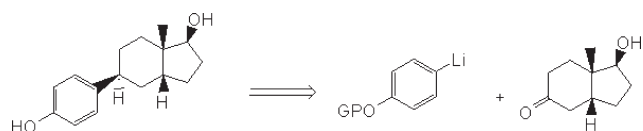


Figure 2. Ring numbering system for estradiol (**E2**) is also used for the A-CD structure, which is shown here with the same chirality as in **E2**.

Scheme 1. Retrosynthetic Analysis of A-CD Ring System Coupling via Li–Carbonyl Coupling to the Saturated CD Ring Moiety



In the present paper we describe a set of A-CD estrogens that is larger than in our previous communication⁴¹ and include details on their synthesis, molecular modeling, relative binding affinities, gene transcription assays, and cytotoxicity. Also, we will point out an incorrect structural assignment in our previous work for the C–D ring junction⁵³ and discuss its significance. The data are examined with respect to two hypotheses: (1) the addition of electron-withdrawing groups on the A-ring will suppress quinone formation, and (2) fluorination at both ortho-positions on the A-ring will retard or even prevent quinone formation. As will be seen, one hypothesis is correct and one is not.

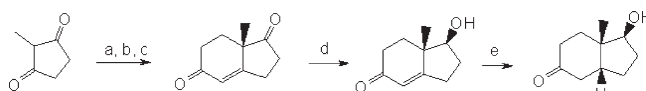
Results

Synthesis of the A-CD Ring Compounds. Figure 2 shows the ring numbering system of estradiol, along with the prototypical A-CD ring system. For convenience in making frequent comparisons to the ABCD steroid structure, we have retained steroid numbering in A-CD even though the B-ring is not present. By use of steroid notation, A-CD can be conceptually made by deletion of carbon atoms 6 and 7 in estradiol. In a 2D drawing the resulting A-CD structure in the natural chirality will overlay exactly over **E2**. In 3D, however, there are important differences, caused by the nearly free rotation about the ring A to ring C bond in the A-CD compounds. Thus, in the free ligands the A–C rings in **E2** are nearly coplanar, whereas in A-CD they are perpendicular.

Our strategy was aimed at creating a family of A-CD analogues. The key target compounds were targeted to have the same absolute stereochemistry as the natural hormone at all centers except C14. The CD ring junction in this series of compounds is *cis* and not *trans* as found in estradiol. Particularly important is the (*S*) stereochemistry at C9. The sequence also yields isomers that have the “non-natural” (*R*), i.e., inverted chirality at C9. However, in this paper we focus only on the analogs with the natural (*S*) configuration at C9.

An overview of the synthetic procedures is as follows: synthesis of the A-CD family of compounds involved coupling of a preformed enantiomerically pure CD ketone with the ring A moiety (Scheme 1). This was most readily accomplished by reaction of the lithiated A-ring, derived by lithium–bromine exchange of an appropriately protected 4-bromophenol with the CD moiety followed by deprotection and adjustments of

Scheme 2^a



^a(a) MVK; (b) (L)-proline/DMF; (c) TsOH/CH₂Cl₂; (d) NaBH₄, MeOH/DMF, –78°C; (e) H₂/Pd.

the functional groups. The precursor A-ring bromides either are available commercially or can be prepared via standard aromatic chemistry.

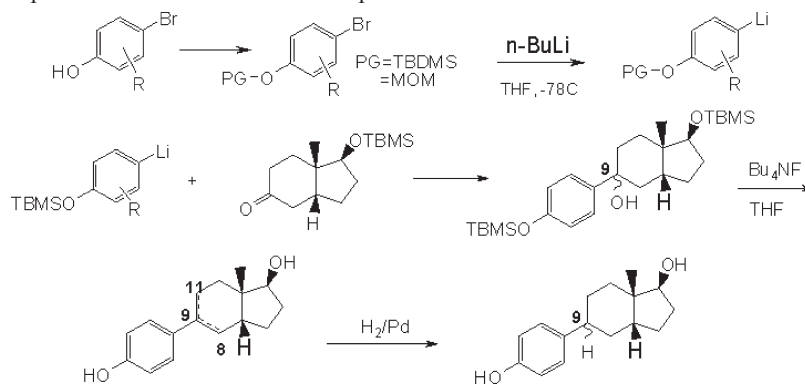
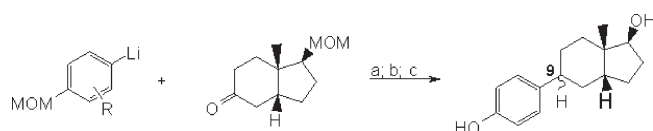
The enantiomerically pure unsaturated CD-ring unit was prepared in multigram quantity following the Hajos–Parrish procedure (Scheme 2).^{54,55} The highly selective reduction of the two carbonyl groups was best accomplished in methanol–CH₂Cl₂ at –78 °C as described by Ward et al.⁵⁶ Further hydrogenation reduces the double bond and gives exclusively the *cis*-fused hydrindane system.

Note that this is different from the *trans*-fused CD system analogous to estradiol (Figure 2), which we assumed would result from the synthesis. However, an X-ray crystallographic determination done on an A-CD derivative (compound **1f**) showed unequivocally that the structure is *cis*, as shown in Schemes 2 and 3 and all figures to follow. We are therefore not simply “deconstructing estradiol” as in the title of our previous communication^{41,53} but rather reconstructing it without the B-ring and with a new stereochemistry in the CD fragment. A literature survey showed that, to the best of our knowledge, the resulting A-CD structure is unique.

Reaction of either TBMS or MOM-protected lithiated ring A with the carbonyl group of the CD-ring component gave typically an 80–90% yield of an almost 1:1 mixture of epimeric tertiary alcohols (Scheme 3). When the hydroxyl protecting group on both rings A and D was treated with TBDMS, Bu₄NF in THF at room temperature afforded a cleanly separable mixture of 9 α - and 9 β -hydroxy isomers. Treatment of the separated isomers or of the mixture with acid gave a mixture of regioisomeric alkenes having the double bond at either C8–C9 or C9–C11. Hydrogenation of this isomer mixture afforded again a mixture of both the 9-(*S*) and 9-(*R*) saturated A-CD ring compounds. These were separated by either silica gel column or preparative HPLC (Scheme 3).

The use of MOM protecting groups allowed us to convert the initial condensation product via acid-catalyzed dehydration and concomitant deprotection directly into the regioisomeric mixture of alkenes; reduction, as before, afforded the mixture of isomeric saturated A-CD compounds (Scheme 4).

In compounds **1a–i** (see Table 1) the isomer that eluted first from the silica gel column was assigned natural 9-(*S*) stereochemistry. This assignment is based on an X-ray structure determination of the faster eluting 5-trifluoromethyl derivative **1f** (Figure 3) which also had by far the higher estrogen receptor binding affinities (RBA α = 89.7, RBA β = 205) compared to the slower eluting isomer. The ¹H NMR and carbon-13 spectra also showed consistent differences with the faster eluting 9-(*S*) isomer showing the C17 hydrogen in the 3.9 ppm range compared to near 4.4 for the 9-(*R*) isomer. The C17 carbon in the ¹³C spectra also showed consistent differences occurring in the 80–83 ppm range for the 9-(*S*) and 73–74 ppm range for the 9-(*R*) isomer. Importantly, the relative binding affinities (RBAs) for the compounds in the 9-(*S*) series were always stronger than those for compounds assigned the 9-(*R*) stereochemistry. Our docking studies also showed clearly that the fit for the 9-(*S*)

Scheme 3. Generation of Separable Mixtures of A-CD Compounds**Scheme 4^a**

^a Reagents: (a) *n*-BuLi, THF/−78 °C; (b) TsOH/MeOH; (c) H₂/Pd.

isomers in the active site should be substantially more favorable than that of the 9-(*R*) derivatives.

By use of these procedures, over 50 novel ligands have been produced, a subgroup of which is reported in this paper. Scheme 5 shows a list of the novel ligands as follows: reference compounds are estradiol, estrone, equilenin, genistein; compounds **1a–o** have natural (*S*) chirality at C9; compound **2** is A-CD with a keto group at C17; **3** has an ethynyl group at C17; **4** and **5** introduce unsaturation into the C-ring. The complete set reported here thus contains 4 reference compounds, 15 novel A-CD compounds where the CD rings are saturated, and 2 compounds with unsaturation in the C-ring. Representative structures and their corresponding numbering scheme are shown in Scheme 5.

Table 1 shows the collected chemical data and some of the biological data for the reference compounds and the novel A-CD compounds that have been synthesized (**1a–o**, **2–5**). This table contains (i) the compound identification number and substitution pattern at positions 2,4,5 on the A-ring, (ii) computed gas-phase bond dissociation enthalpy (BDE) of the phenolic OH at C3 in the free ligand, (iii) interatomic distance R_{O-O} between terminal oxygen atoms at C3 and C17 in the free ligand, (iv) interatomic distance R_{O-O} between terminal oxygen atoms at C3 and C17 in the bound ligand, (v) A-C twist angle τ_L of free ligand, (vi) A-C twist angle τ_R of ligand in the best docked pose in the complex, (vii) experimental relative binding affinity (RBA) values for binding of ligand to receptors ER α and ER β and the β/α ratio, and (viii) experimental relative transcription activation (RTA) values for activation of the estrogen response element (ERE) by ligand-activated ER α or ER β and their β/α ratio. For details of the procedures used to obtain these values, see the Experimental Section.

To understand Table 1, the conformational possibilities and the twist angle mentioned previously require some clarification. Figure 5a shows compound **1c** in its lowest-energy (perpendicular) conformer, Figure 5b in the coplanar potential maximum configuration, and Figure 5c in the secondary (perpendicular) potential minimum. The two minima can be denoted 5-F A-CD and 1-F A-CD. Since it is usually true that the lowest conformer has the substituent opposite the

methyl group at C13, we will adopt a notation consistent with this idea (i.e., R2 = H, R4 = H, R5 = F). The twist angle is taken as the numerical average of the two sets of four atoms defining the A-C dihedral angle. When F is antiparallel to methyl (Figure 5a), $\tau = -90^\circ$; rotation of the A-ring in the direction shown makes the system coplanar (**5b**) where $\tau = 0$ deg and then perpendicular again with F parallel to methyl (**5c**) where $\tau = +90^\circ$ (Figure 4). The limits of the twist angle are thus from -180° (F-atom closest to methyl) to $+180^\circ$. When both ortho- and meta-substituents are present on opposite sides of the phenolic OH, the meta-group takes priority in the definition.

Discussion

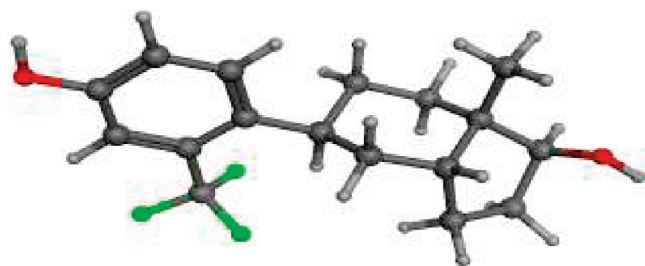
Overview of Trends in Binding Affinity. Compounds **1a–o** show a range of RBAs varying from almost zero (**1h**) to very strong (**1c**, **1d**, **1f**). On going from 17 β -OH to 17-keto, there is a significant drop in binding affinity; compare **E2** to **E1** (100:4), and **1a** to **2** (1.47:0.008 for ER α , 21.5:0.11 for ER β). This is even more significant for the A-CD compounds (factor of ~ 200) than for the ABCD reference compounds (factor of 25).

Ortho-fluorination (e.g., as in **1b** vs **1a** where ortho and meta are defined relative to the 3-hydroxy substituent) causes a drop in RBA by about a factor of 2, whereas when both ortho-positions are fluorinated (**1g** vs **1a**), the drop in RBA is much larger (factor of 50), since the 2-position interacts with both hydrogen bonding residues [Arg394, Glu353 in ER α] while the 4-position interacts only with one [Arg394]. *Meta*-substitution, on the other hand, can strongly increase the RBA. For example, for ER α compare **1a** (H, RBA = 1.47) to **1c**, **1d**, **1e**, **1f** (F, Cl, Me, CF₃), giving 27.3%, 52.3%, 2.82%, and 89.7%, respectively. For ER β the same comparison gives the following: **1a**, 21.5; **1c**, **1d**, **1e**, **1f**, 136%, 168%, 33.6%, 205%). From this group compounds **1d** (or 5-Cl A-CD) and **1f** (or 5-CF₃) have among the highest RBAs of any compound in this paper (ER β 168% and 205%, respectively). By contrast, 2,4-dichloro A-CD, **1h**, has an almost negligible RBA for both receptors, emphasizing the importance of the size and location of the functional groups on the A-ring. Compounds **4** and **5**, with a conjugated double bond in the C-ring, mostly exceed the RBAs of **E2**. In comparison with the corresponding saturated compound (**1d**), compound **4** binds more strongly to both receptor subtypes. Thus, unsaturation can be a desirable feature, and a larger set of compounds containing this feature will be discussed in a future publication.

Table 1. Compound Numbers As Shown in Scheme 5^a

compd	BDE	R _{O–O} free	R _{O–O} ER α	τ_L free	τ_R ER α	RBA (ER α)	RBA (ER β)	RBA (β/α)	RTA (ER α)	RTA (ER β)	RTA (β/α)
estradiol (E2)	85.5	10.98	11.13	−4.8	−4.5	100	100	1.00	100	100	1.0
estrone (E1)	85.7	10.87		−4.4		4.5 ± 0.7	3.8 ± 0.4	0.84			
equilenin	83.7	10.83		+0.6							
genistein	86.1	12.04		+49.9		0.019 ± 0.004	7.42 ± 0.50	391			
1a H H H	85.2	10.78	11.15	−88.9	−60.7	1.47 ± 0.26	21.5 ± 4.6	14.6	4.2 ± 3	164 ± 2	39
1b F H F	86.2	10.78	11.13	+88.3	−65.6	1.04 ± 0.20	8.68 ± 1.7	8.3	−9.0 ± 9	196 ± 3	pure β
1c H H F	86.2	10.78	11.15	−88.6	−60.4	27.3 ± 0.69	136 ± 7.3	5.0	44.3 ± 12	158 ± 1	3.6
1d H H Cl	86.3	10.76	11.17	−85.2	−56.9	52.3 ± 12	168 ± 33	3.2	90 ± 13	189 ± 7	2.1
1e H H Me	85.1	10.76	11.16	−88.0	−60.3	2.82 ± 0.45	33.6 ± 6.2	11.9	−9.7 ± 3	49.2 ± 10	pure B
1f H H CF ₃	87.1	10.75	10.94	−92.5	−106.2	89.7 ± 14	205 ± 23	2.3			
1g F F H	84.8	10.77	11.13	−86.6	−62.2	0.040 ± 0.002	0.277 ± 0.006	6.9			
1h Cl Cl H	85.8	10.78	9.93	−87.0	−80.3	0.004 ± 0.001	0.002 ± 0.001	0.5	0.0 ± 4	0.0 ± 3	
1i H F F	87.2	10.79	10.99	+88.8	−109.3	4.62 ± 0.93	42.8 ± 5.5	9.3	18.3 ± 4	151 ± 1	8.3
1j F H F	86.5	10.78	10.98	−87.9	+75.3	0.38 ± 0.09	3.3 ± 0.7	8.7			
1k F F F	85.5	10.77	11.13	−85.7	−62.3	0.186 ± 0.01	1.73 ± 0.2	9.3	12.8 ± 0.4	95.4 ± 4.0	7.9
1l H Me F	83.9	10.78	11.03	−88.5	−32.9	1.75 ± 0.50	1.75 ± 0.51	1.0			
1m ^b H Cl H	87.1	10.75	10.69	−87.4	+52.1						
1n ^b Cl H Cl	88.1	10.77	10.93	112.9	+73.1						
1o H Me Me	82.7	10.76	10.81	−79.6	−115.4	0.065 ± 0.001	0.183 ± 0.05	2.8			
2 A-CD keto		10.86	10.82	−87.2	−101.5	0.008 ± 0.001	0.112 ± 0.01	14			
3 A-CD 17-C2H		10.72	10.58	57.7	−49.5	0.088 ± 0.006	0.110 ± 0.03	1.3	−16.9 ± 3	35.9 ± 2	Pure β
4 5-Cl Δ C8,C9		10.83		−46.5		195 ± 35	331 ± 25	1.7	98.6 ± 5.5	126.7 ± 7.9	1.3
5 5-Cl Δ C9-C11		10.84		+47.5		51.9 ± 7.9	118 ± 4	2.3	114.6 ± 2.9	116.8 ± 7.8	1.0

^a Units: BDE in kcal/mol, R_{O–O} in Å, τ in deg. ^b These compounds were not synthesized and are included for theoretical discussion.

**Figure 3.** Structure of compound **1f** as determined by single crystal X-ray structure determination.

The twist angle in the free ligands **E2**, **E1**, and equilenin is near zero because of the constraint arising from the B-ring. Genistein, on the other hand, is free to twist, and the resulting dihedral angle is 50°. The twist angle for most of the free ligands (i.e., **1a–o**) is nearly perpendicular at $-90^\circ \pm 5^\circ$. Compound **3** containing the 17-ethynyl group is notably different at $+57.7^\circ$.

When the ligands are docked into the receptor, there is a grouping of docked ligands with twist angle near -60° (**1a–e**, **1g**, **1k**) and another group near -105° (**1f**, **1j**, **1n**, **1o**, **2**). The first group is twisted by 30° relative to the free ligand and the second group by only 15° .

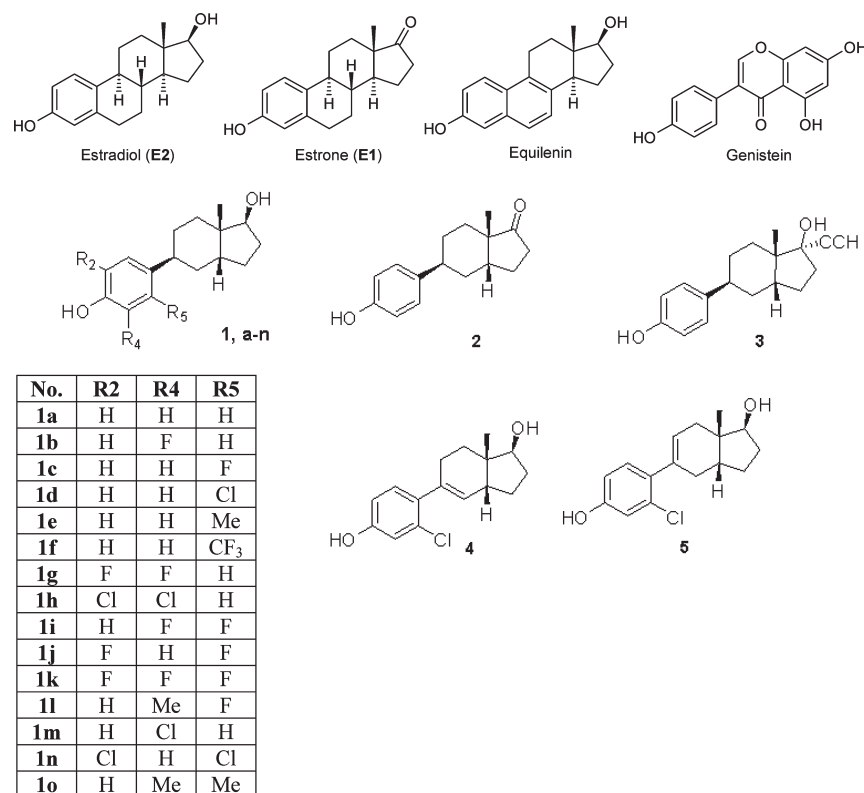
Selectivity of the ligands for ER α or ER β is expressed in Table 1 as the RBA ratio β/α . Restricting attention to compounds **1a–o**, essentially all compounds are ER β -selective; e.g., the unsubstituted **1a** has ratio $\beta/\alpha = 14.6$. Substituents added to the A-ring all reduce the selectivity. In one case (**1h**), the selectivity is so reduced that it becomes ER α -selective with ratio $\beta/\alpha = 0.5$, although this compound also has very low RBA values.

RTA values generally track RBA values; i.e. a high binding affinity is required to cause significant gene transcription. An important observation, however, is that the correlation is very nonlinear.

BDE Values and Quinone Formation. One mechanism for estrogen catechol and eventually orthoquinone metabolite

formation begins with abstraction of the most weakly bonded H-atom. The aromatic O–H bond at C3 is much weaker than the O–H bond at C17, and abstraction to form the phenoxyl radical may be followed by P450-catalyzed hydroxylation at the adjacent ortho-site with subsequent rearrangement to form the catechol. As discussed above, catechol formation then leads to formation of cytotoxic quinones. Therefore, according to our first hypothesis, the stronger is the O–H bond, the slower will be the rate of catechol formation. Table 1 shows the OH BDE values for all compounds in this study from our DFT calculation, which gives a BDE for phenol of 87.4 kcal/mol (exptl, 87.5 ± 1 kcal/mol).⁵⁷ The appropriate reference compound for comparison is **E2**, with a BDE of 85.5 kcal/mol. The lowering in BDE for **E2** relative to phenol is essentially caused by a para-alkyl electron donor (-2 kcal/mol) and a meta-alkyl electron donor (about -0.3 kcal/mol).^{58,59} Thus, because of a lower BDE, **E2** should show a somewhat stronger tendency toward quinone formation than phenol.

To illustrate this point, equilenin has a lower BDE (83.7) than **E2**, caused by the radical stabilization coming from the second aromatic ring. This appears to be sufficiently below the BDE of **E2** that it may be responsible for the significant increase in tumor promotion for equilenin.¹³ Similarly, compounds that have a double bond conjugated to the phenol ring have relatively low BDEs.⁵⁸ However, the presence of strongly electron-withdrawing groups such as $-\text{CF}_3$ or $-\text{CN}$, particularly in the meta-position (**1f**, 87.1 kcal/mol), can significantly increase the BDE. Many of the compounds in Table 1 have BDE values higher than **E2** because of the presence of these electron-withdrawing groups, and according to the phenoxyl radical mechanism, the differences in rate of quinone formation may be very sensitive to these small variations.^{60,61} As a rough guide then, we are looking for compounds with a BDE greater than that for **E2**. The relationship to quinone toxicity^{13,62–64} will be discussed in more detail in the next section, using a subset of the data in Table 1.

Scheme 5. Numbering Scheme for A-CD Compounds^a

^a Substituents on **1a–o** are in the order R2, R4, R5, where R2 = substituent located at position 2 in A-ring, R4 = substituent at position 4, etc. If R5 = H, due to free rotation of the A-CD twist angle, R2 and R4 are equivalent.

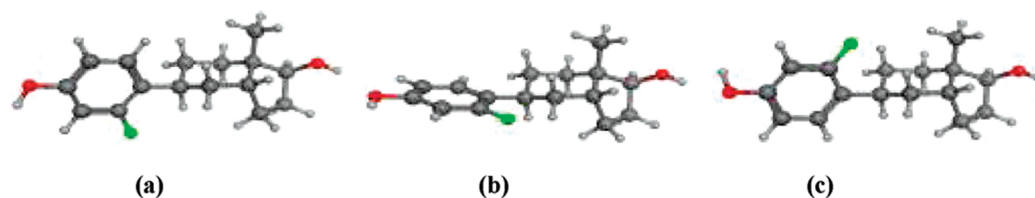


Figure 4. Definition of the A-C twist angle, using compound **1c** as an example: (a) -90° ; (b) 0° ; (c) $+90^\circ$.

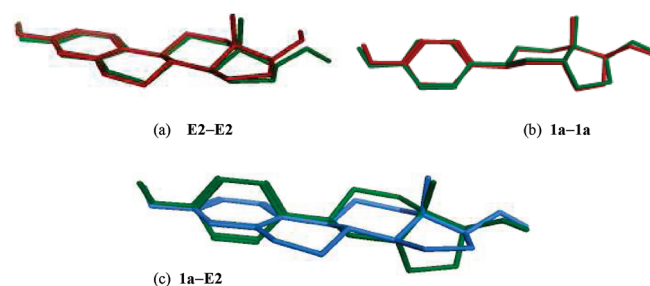


Figure 5. (a) Superposition of **E2** showing the free ligand (red) and the best docked structure (green). (b) Superposition of **1a** showing the free ligand (red) and the best docked structure (green). (c) Superposition of docked **1a** (green) over docked **E2** (blue).

Oxygen–Oxygen Interatomic Distances. Figure 5a shows a picture of the lowest-lying conformer of **E2** (in red) superposed over its best docked structure (green). Although the differences are small, the docked structure is flattened slightly, causing the O–O distance to increase from 10.98 Å (free ligand) to 11.13 Å (bound complex), i.e., an increase of 0.15 Å. Figure 5b shows the same superposition for **1a**, where the increase is larger, from 10.78 to 11.15 Å (0.37 Å). This is

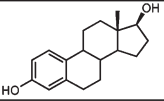
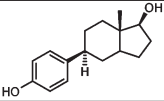
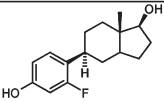
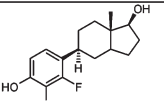
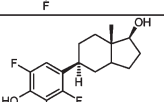
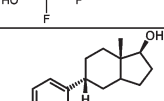
accomplished mostly by an adjustment in the position of the ring D. Table 1 shows that this is a common phenomenon, with eight of the compounds having docked structures with O–O distances near 11.15 Å. Compound **1h** is an exception; here the bond distance goes from 10.78 (free) to 9.93 Å (bound). Notably, **1h** also has the weakest RBA of any compound in Table 2.

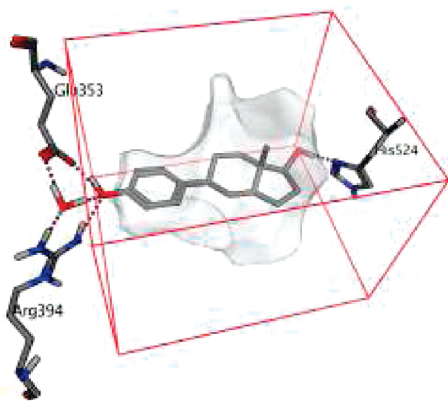
Figure 5c shows an overlay of **E2** (blue) and **1a** (green). The main differences are the twisting around the A–C bond in A-CD, the absence of the two B-ring carbons in A-CD, and the different projection angles of the two cyclopentane rings. Remarkably the O–H bonds in the two structures are almost superposed.

Considering the main A-CD series **1a–o**, the O–O distance for the ligand in the bound complex is significantly longer than for the free ligand. This lowers the energy of the complex by moving down the attractive wall of the H-bond potential, which compensates for the rise in potential caused by twisting the ligand.

Docking. The docking procedure was carried out as described in the Experimental Section. The force field chosen for this study was MMFF94s, an option available in MOE. By use of the MOE software, a docking box was chosen as

Table 2. Hepatocyte Toxicity, Showing LC₅₀ for 2 h of Exposure, and BDE and Calculated log *P*

Compound	Structure	Hepatic Cell LC ₅₀ (μM)	BDE (kcal/mol)	ClogP
E2		400-450	85.5	3.91
1a		320-400	85.2	3.59
1c		250-280	86.2	3.75
1i		155-200	87.2	3.91
1k		>600	85.5	4.06
Enantiomer of 1a		300-350	85.2	3.59

**Figure 6.** Docked structure of compound **1a** in cavity of hERα: receptor cavity, gray surface; docking box, red lines; main pharmacophore residues, gray; H-bonds, dotted lines. Other residues are hidden for clarity.

described in Experimental Section and the interaction surface rendered. Figure 6 shows the result for the parent compound **1a** in its lowest-energy bound conformation. The figure shows that the phenolic H-bond at C3 also includes a bridging water molecule between the ligand and the residues Arg394 and Glu353. This is consistent with the known crystal structure of **E2** in human ERα (hERα).⁶⁵

For the dissociation reaction complex → ligand + receptor (C → L + R) with dissociation constant K_d , a full theoretical treatment, including all enthalpy and entropy changes to obtain the free energy change $\Delta G^\circ = -RT \ln K_d$, would be prohibitively difficult. This is not only due to the sheer size of the system but also due to its complexity. For instance, in the receptor prior to ligand binding there are ~10 water molecules that interact with each other and with the receptor cavity walls according to a potential function which would be different from that of a water

molecule interacting with continuum water solvent. On the other hand, many terms will be essentially constant over the series of ligands: e.g., the energy of the free receptor (E_R) is rigorously constant. This is also approximately true for the complex, since its exterior surface should not change appreciably when a ligand is bound.

In the spirit of attempting to calculate ΔG° , only energy-based terms were chosen as descriptors. In the force field model, the total energy of a bound complex AB is separable in terms of its components A and B, i.e., $E_{AB} = E_A + E_B + E_{int}$, where E_{int} is the interaction energy between A and B, which includes only nonbonded interactions. Initially, a multiple linear regression model was used to correlate the experimental RBAs with a chosen set of descriptors. These consisted of (i) the energy of R in C (E_R') relative to a reference value of 330 kcal/mol, i.e., $\Delta E_R = E_R' - 330$, (ii) the interaction energy between L and R in C (E_{int}), (iii) the deformation energy of L, i.e., $E_L' - E_L = \Delta E_L$, and (iv) the solvation energy of the free L, ΔE_{solv} .

Briefly, the docking procedure described in the Experimental Section involves generation of a conformer list for each ligand, generating and docking 90 poses per conformer, assigning a scoring function (SF) with equal weights to the four variables described above, rank-ordering the poses according to the initial SF, choosing the best pose for each ligand, running a multiple linear regression in each independent variable (the dependent variable is the experimental log of RBA) to obtain a predicted value for log RBA, determining the weight of each variable in the SF, rank-ordering the poses again, and iterating to self-consistency. Surprisingly, the variables ΔE_L and ΔE_{solv} did not contribute significantly to the SF and were omitted. However, the use of the remaining two variables ΔE_R and E_{int} and the procedure described above resulted in high-quality correlations for both ERα and ERβ.

The following regression equations were obtained for the set of A-CD compounds, which included compounds **1a–o** (excluding **1m** and **1n** for which no experimental data were available) and compounds **2** and **3**. These can be strictly considered as the “training sets” for each receptor subtype. However, the cross-correlation coefficient Q^2 , based on the “leave one out” method, also gives an indication of the robustness of the fit (a measure of its ability to fit other related structures).

For ERα,

$$\text{predicted log RBA} = (-19.80 \pm 1.46) - (0.3105 \pm 0.0195)E_{int} - (0.0530 \pm 0.0085)\Delta E_R \quad (1)$$

where $n = 15$, $R^2 = 0.97$, standard deviation is 0.26 log unit, $Q^2 = 0.95$, and there are no outliers.

For ERβ,

$$\text{predicted log RBA} = (-21.32 \pm 3.51) - (0.3207 \pm 0.0468)E_{int} - (0.00418 \pm 0.0083)\Delta E_R \quad (2)$$

where $n = 12$, $R^2 = 0.90$, standard deviation is 0.53 log unit, $Q^2 = 0.69$, and one outlier is removed.

The quality of the fits for eqs 1 and 2 is shown graphically in Figure 7. Figure 7a shows an excellent fit to the training set (A-CD compounds, ERα), with a standard deviation of only 0.26 log unit. Figure 7b also shows a good fit to the training set of A-CD compounds for ERβ. To test the predictive value of the fitting functions using data outside the A-CD training set, and for which RBA data are known, we looked at the ERα correlation and extended it to include the data for estradiol (**E2**), estrone (**E1**), and genistein (**GS**). For the ERβ correlation, we added just one point, **E2**. Both **E2** and **E1** have a

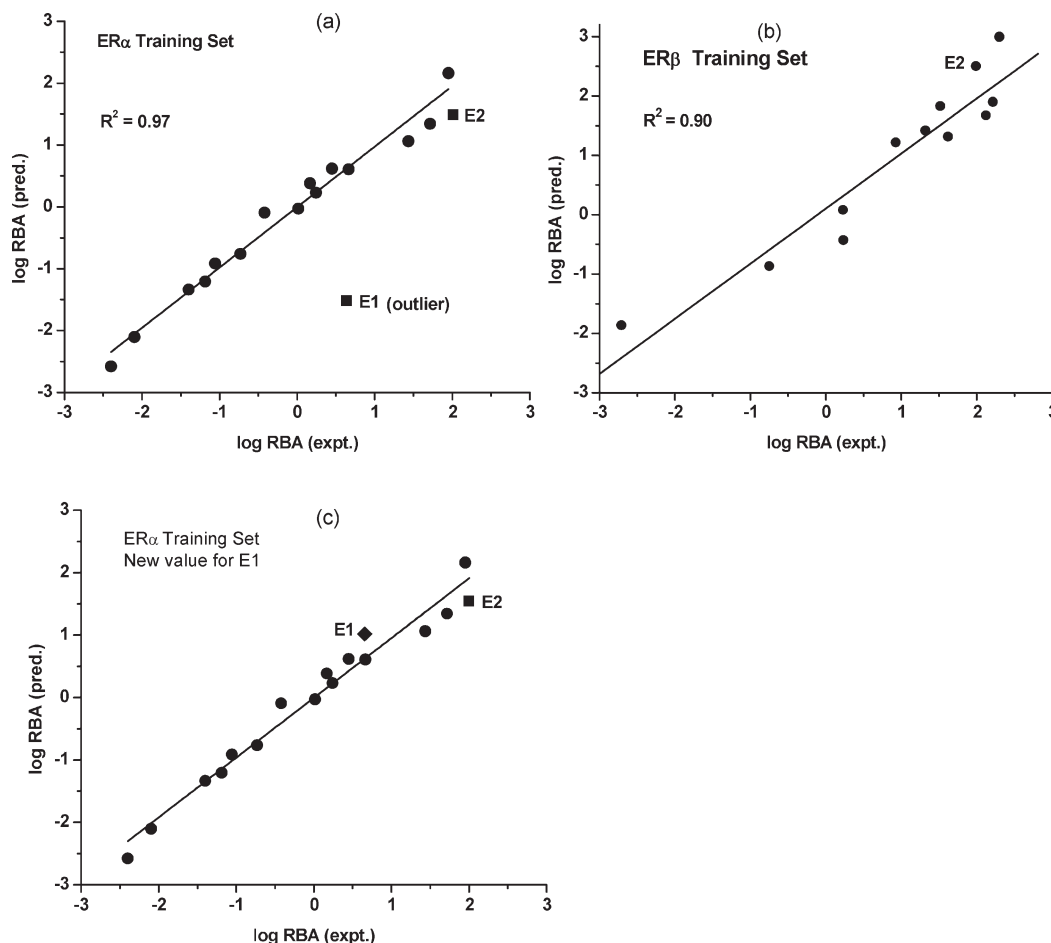


Figure 7. The log of the predicted and experimental binding affinities for A-CD compounds. (a) ER α training set: $n = 15$, $R^2 = 0.97$, std dev = 0.22 log unit, $Q^2 = 0.950$, no outliers. Test Set: **E1** and **E2**. (b) ER β training set: $n = 12$, $R^2 = 0.89$, std dev = 0.40 log unit, $Q^2 = 0.77$, one outlier removed. (c) ER α training set as in (a), with new value for **E1**.

close resemblance to the A-CD series except for the fact that both the free ligand and bound ligand are nearly planar rather than strongly twisted. **GS**, on the other hand, is rather different, with its strong polarity and rather long oxygen–oxygen distance of 12.04 Å. So it was not surprising that eq 1, which does not include a term for solvation energy, was useless at predicting the RBA for **GS**, which is an outlier by more than 4 log units.

When constants from eq 1 are used, the quality of the overall fit, including the additional points for **E1** and **E2**, is very good for **E2** (deviation of <0.1 log unit) but **E1** is a strong outlier with a predicted log RBA that is too low by a full 2.0 log units (see Figure 7a). This is far outside the standard deviation of the fit from eq 1 (0.26 log unit). Figure 7b shows that **E2** is also well fitted using constants from eq 2.

We were puzzled by the fact that **E2** was well fitted in both correlations but **E1** was not, and we looked into the cause of this problem. After some study we discovered that because of the rigid near-planarity of **E1**, the hydrogen bond at the C17 carbonyl group was lost, i.e., His524 was not acting as a donor to the carbonyl acceptor, so the RBA was significantly underestimated. Introduction of a second bridging water molecule between the oxygen at C17 and His524 allowed the H-bond to re-form with the result that the predicted RBA for **E2** now exceeded the experimental value by 0.14 log unit, i.e., well within the standard deviation of the fit (the result is shown graphically in Figure 7c). We were not able to find a structure for estrone bound to ER α in the Protein Data

Base, but it would be interesting to test this prediction experimentally.

Factors Affecting Binding Affinity: Residue Interactions.

Figure 8 shows a comparison of the absolute interaction energies of **E2** and **1a** with the active site residues. The differences are subtle and are more visible on a difference map of **E2** – **1a**, shown in Figure 9. The positive values in this figure denote weakened interactions for **1a** vs **E2**; negative values show strengthened interactions. The hydrogen bonding interactions come from the residues Glu353, Arg394, His524, which do not change appreciably (<1.0 kcal/mol). The most noticeable variations are the weakened interactions with Leu384, Met388, Leu525, all of which are hydrophobic interactions (Leu384 and Met388 near the B-ring of **E2**, Leu525 near the methyl group). Because the B-ring is not present in **1a**, it is reasonable to expect such weakening. On the other hand, some interaction are strengthened, notably those with Arg394 and Met522.

The residue-by-residue analysis generates so much data that it is hard to interpret in terms of useful drug design input. Therefore, we decided to group the interactions so that we could analyze contributions to stabilization of the individual moieties of the reference compound. For this we chose the rings A, B, C, D, the 13-methyl group, and the two hydrogen bonds at C3 and C17. For example, the A-ring of estradiol closely interacts with the residues located within 3.5 Å, which are denoted as “group A” residues. The sum of the interaction

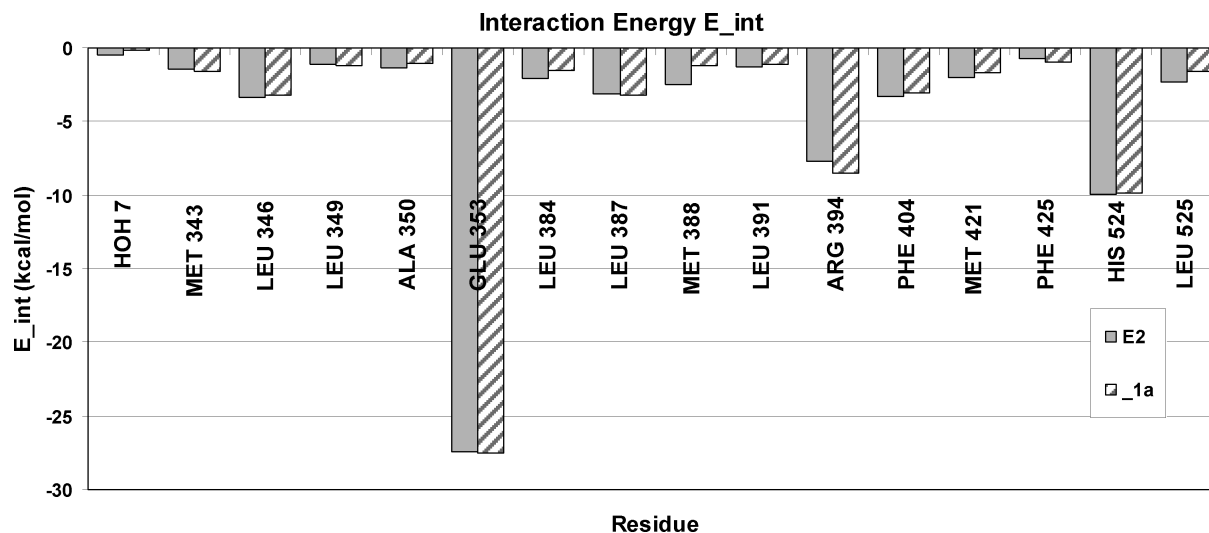


Figure 8. Interaction energies of the active site residues with **E2** (slanted bars) and **1a** (solid). All values are in kcal/mol.

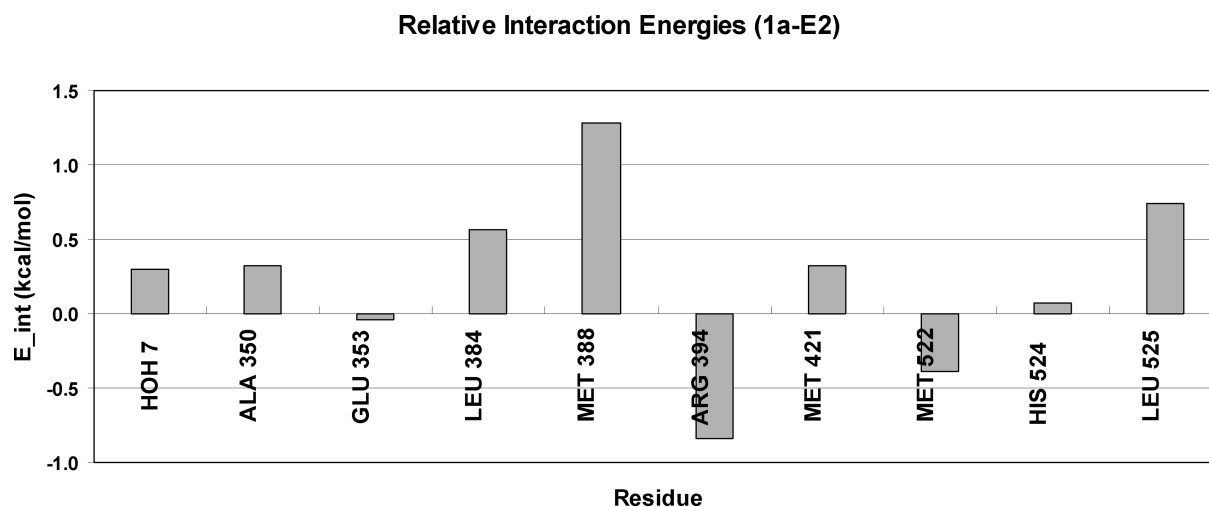


Figure 9. Difference map of interaction energies of **1a** relative to the reference compound **E2**. All values are in kcal/mol.

energies of each ligand with all groups of residues in this way is shown in Figure 10 for compounds **1a**, **1d**, and **1e**.

Figure 10a shows more clearly that the interactions with the B- and C-ring residues have been significantly weakened in **1a**, consistent with the low binding affinity measured for ER α (1.5%). The interactions with the A and D rings have also been weakened, although less so. Only the hydrogen bond at C3 has been strengthened and only slightly. Such a detailed analysis offers a unique insight that allows for understanding of the drug–target interactions and leads to specific suggestions on how to improve the binding.

Table 1 shows that the meta-substituents improve the binding affinity. The reason for this activating effect can be seen from the residue analysis. Figure 10b shows the 5-Cl A-CD interaction profile. From this figure, it is clear that the interactions of the ligand with the B-ring residues are restored in **1d**. Also the interactions of the A-ring residues and the C3 hydrogen-bonding residues are improved for this compound. Closer examination of the geometry reveals that this is due to slight movement of the A-ring toward those residues. In other words, the activating effect of 5-substituents is due to hydrophobic interactions with the B-ring residues, as well as insertion of the A-ring toward the neighboring residues, which improves the hydrophobic and van

der Waals interactions. Larger substituents on C5, however, are in general not well tolerated, particularly if they are very non-polar. As shown in Figure 10c, the 5-methyl group in **1e** is large enough to cause steric clashes with B, C, and D group residues, thus resulting in a lower binding affinity to ER α for this compound (RBA = 2.8%). Polarity also plays a role, since the 5-CF₃ A-CD (**1f**) has a high RBA of 89.7%.

Origins of Selectivity. For the compounds **1a–o**, the highest selectivity in RBA is obtained for **1a** ($\beta/\alpha = 14.6$). According to Figure 10a, the most significant changes in the residue interactions of this compound vs **E2**, where $\beta/\alpha = 1$, are the weakening of the B-ring interactions. Moreover, when these interactions are restored in **1d** through 5-chloro substitution, the selectivity is significantly decreased ($\beta/\alpha = 3.2$). When the discussion is limited to A-CD compounds a simpler argument is applicable: the A-CD compounds are generally smaller than **E2** (calculated van der Waals volumes: **E2**, 283 Å³; **1a**, 258 Å³). Thus, because of the smaller size of the ER β cavity, they are better tolerated by the ER β receptor. Predictably, the larger A-CD compounds tend to lose their ER β selectivity (**1d**, 273 Å³; **1e**, 277 Å³).

RTA Values. As stated previously, we expected there to be a significant correlation between the binding affinity of a

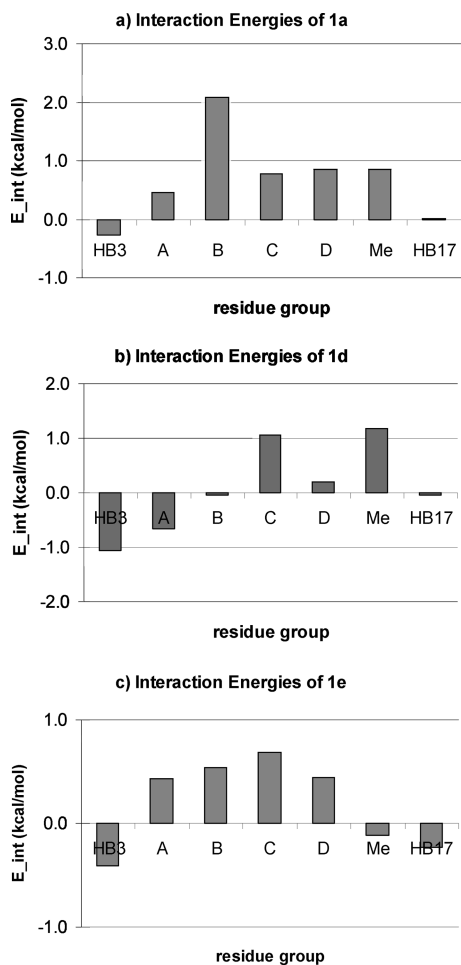


Figure 10. Interaction energies of some A-CD compounds relative to the reference compound **E2**. All values are in kcal/mol. Receptor is ER α . (a) Interaction energies of **1a**. (b) Interaction energies of **1d**. (c) Interaction energies of **1e**.

ligand to its receptor and the corresponding transcriptional activation. Table 1 shows that the compounds with the highest RBAs for ER α also have the highest RTAs, e.g., compound **1c** (RBA = 27%, RTA = 44%) and compound **1d** (RBA = 52%, RTA = 90%). The same is true for ER β , e.g., for **1c**, **1d**, and **1e** RBAs are 136%, 168%, and 34% whereas RTAs are 158%, 189%, and 149%. Since binding affinity is measured by the free energy change $\Delta G^\circ = -RT \ln K_d = -2.303RT \log K_d$, it is appropriate to use log RBA in such correlations. On the other hand, there is nothing inherently logarithmic about transcription activation and very small values (< 1%) cannot be measured accurately, so we chose to correlate RTA with log RBA.

Figure 11 shows the correlation between RTA and log RBA for ER α and ER β using data from this study. Figure 11a shows the result for ER α , where a sigmoid-type function has been fitted to the data. Figure 11b shows that a sigmoid-type function also fits the data for ER β . Similar observations were made on RBA and RTA for values previously published.^{30,66} Other studies have noticed the cooperativity of ligand-binding with downstream events including dimerization and DNA binding.^{67,68} A very recent study by Bourgoin-Voillard et al.⁶⁹ on coactivator recruitment and transcription activation for ligand-activated ER α also showed sigmoidal-type plots of coactivator binding vs log of the concentration of ligand. This intriguing and “steep” relationship between RTA and log RBA

deserves further investigation, but it suggests that the functional selectivity of a particular ER ligand for ER α or ER β might be greater than its binding selectivity for the two ER subtypes. Thus, the search for ligands that have extreme ER subtype binding selectivity may be unnecessary if the aim is to achieve effective functional selectivity.

Toxicity and Quinone Formation. As discussed in the Introduction, when quinones are present, they increase the toxicity to cells by three mechanisms: redox cycling which generates superoxide radicals and hence causes oxidative stress, thiol depletion which upsets the cellular redox balance, and formation of DNA adducts which can lead to mutations during cell replication. We examined the cytotoxicity using hepatocytes where LC₅₀ values were determined after 2 h, using trypan blue indicator.

Results from this assay are shown in Table 2, which also contains the phenolic OH BDE and the calculated octanol–water partition coefficient, ClogP. Data are given for estradiol and four compounds from Table 1, as well as the enantiomer of **1a**. As a control, **E2** has an LC₅₀ in the range 400–450 μ M. Under the conditions of this assay, **E2** is known to undergo quinone formation, which contributes to the toxicity. We confirmed this in our own experiments by adding dicoumerol, a known inhibitor of quinone reductase (which converts the quinone back to the catechol), and observing a marked increase in **E2** cytotoxicity (data not shown).

First, consider the overall trends. Compound **1a** is slightly more toxic than **E2**, and its enantiomer possesses comparable toxicity. As fluorine atoms are added in **1c** (meta-F) and **1i** (ortho, meta-diF), the hepatotoxicity increases substantially, with LC₅₀ values decreasing to about 275 and 180 μ M, respectively (mean values). There is not much variation in BDE for the compounds in Table 2 (from 85.2 to 87.2 kcal/mol), but according to our earlier discussion, compounds with lower BDE should be more toxic. This is clearly not the case, since compound **1i**, which has the highest BDE (87.2 kcal/mol), also has the highest toxicity (LC₅₀ = 155–200 μ M). On the other hand, it was found previously by O’Brien and co-workers⁷⁰ that increasing values of log *P* led to an increase in toxicity. Comparing the series **1a**, **1c**, and **1i** with 0, 1, and 2 F-atoms on the A-ring, it can be seen that toxicity does indeed increase with ClogP. Therefore, we would expect **1k**, with 3 F-atoms and the highest ClogP in the table (4.06), to be very cytotoxic. On the contrary, compound **1k**, i.e., 2,4,5-triF A-CD, is the least toxic compound in the table, with an LC₅₀ above the range of our assay (> 600 μ M). These data show that when ortho-positions are vacant, then hydroxylation and subsequent quinone formation can occur even when an electron-withdrawing group is present in the meta-position but that occupying both ortho-positions by a substituent, even one as small as an F-atom, effectively prevents enzymatic hydroxylation. In other words, they strongly indicate that our first hypothesis, the protective effect of higher BDE compounds containing electron-withdrawing groups, is wrong but that the second hypothesis, on the protective effect of blocking the ortho-positions, is correct. More recent data we have been accumulating will reinforce these conclusions.⁷²

Summary

An easy way to accomplish ring substitution on **E2**-related estrogens is to modify the A-ring separately and then connect to the CD fragment with the Hajos–Parrish ring coupling reaction. Using this procedure, we prepared a variety of A-CD estrogens. These compounds have a different stereochemistry

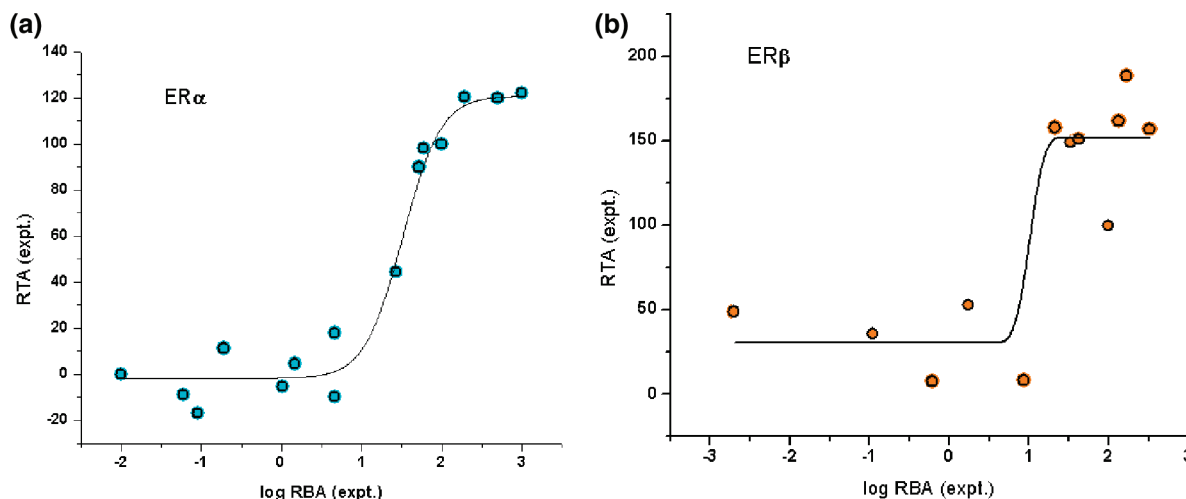


Figure 11. Relative transcription activation (RTA) in the estrogen response element as a function of the log of the relative binding affinity (log RBA) for (a) ER α and (b) ER β .

at the C13–C14 bond from **E2**, where they are cis instead of trans. Relative binding affinities were measured for these compounds for the two estrogen receptors ER α and ER β . A wide range of RBAs was observed ranging from 15-fold selective for ER β to 2-fold selective for ER α . In general, ortho-substitution on the A-ring decreases binding affinity whereas meta substitution increases it. Some compounds (containing F, Cl, CH₃, and CF₃) have binding affinities comparable to or higher than that of the reference compound estradiol. Transcription activation for the estrogen response element was measured and found to correlate with (log) RBA by a sigmoid type function. On the basis of the RTAs, some compounds were pure ER β agonists.

Trends in RBA were discussed using BDEs, twist angles, docking results, and a residue interaction energy analysis. The experimental RBA values were well correlated using only two variables, the interaction energy and the receptor deformation energy, giving a correlation coefficient $R^2 = 0.97$. Genistein could not be fitted using this correlation function, but estradiol was well fitted for both ER α and ER β . Estrone was also well fitted in ER α , provided that an extra bridging water molecule was introduced into the receptor. Hepatocyte toxicity was used as a measure of the tendency to form quinones. Some members of the A-CD series were more toxic than estradiol, probably because of their increased lipophilicity. A notable exception was the 2,4,5-trifluoro A-CD, where both ortho positions are blocked. Thus, our first hypothesis that addition of electron-withdrawing groups on the A-ring would suppress quinone formation appears to be wrong, whereas the second hypothesis that fluorination at both ortho-positions on the A-ring would suppress quinone formation appears to be correct. The 2,4,5-trifluoro A-CD and related compounds are now undergoing more advanced testing. Preliminary results, to be reported in future publications, show that these compounds are metabolically stable and thus show promise for purposes of hormone replacement therapy.

Experimental Section

Synthesis. General Methods. All moisture-sensitive reactions were carried out under nitrogen atmosphere. Anhydrous solvents were obtained as follows: THF, Et₂O, distilled from sodium and benzophenone; CH₂Cl₂ distilled from CaH₂. Analytical TLC was performed with 0.25 mm silica gel 60F plates with 254 nm fluorescent indicator from Merck. Plates were

visualized by ultraviolet light and treatment with acidic ceric ammonium nitrate or potassium permanganate stains followed by gently heating. Silica gel 60, (40–60 μ m) was purchased from Aldrich. The ¹H NMR and ¹³C NMR were recorded on Bruker Avance 500, 400, and 300 spectrometers. Mass spectrometry (MS), using either electron impact (EI) or chemical ionization (CI), was performed on a V. G. Micromass 7070 HS mass spectrometer with an electron beam energy of 70 eV (for EI). High-resolution mass spectrometry (HRMS) was performed on a Kratos Concept-11A mass spectrometer with an electron beam of 70 eV or a JEOL double focusing magnetic sector mass spectrometer JMS-AX505H. All compounds reported were purified via silica gel column chromatography or by preparative HPLC. On the basis of integration values, the purity of all compounds is estimated at >98%.

The CD ring dienone **A** was prepared in highly enriched enantiomeric form following the procedure of Hajos and Parrish.^{54,55} We found the Ward modification^{56,71} for the reduction of **B** to the enone **C** (NaBH₄ in a 1:1 mixture of methanol and dichloromethane) more reliable than the original Hajos–Parrish procedure. Reduction of **C** with H₂/Pd afforded the saturated keto alcohol **D**.

Protection of the Hajos–Parrish Ketone as Its TBMS Ether. To a solution of the Hajos–Parrish ketone (17.85 mmol) in dimethylformamide (20 mL) were added imidazole (35.7 mmol) and TBDMSCl (19.23 mmol). The reaction mixture was stirred at room temperature for 1 h. The reaction mixture was diluted with EtOAc and washed with water and brine. The organic layers were combined, dried over MgSO₄, filtered, and concentrated in vacuo. The crude yellow oil was purified on a silica column. Purification of crude product afforded the desired product as a clear oil in 90% yield. ¹H NMR (300 MHz, CDCl₃) δ 3.80 (t, $J = 4.8$ Hz, 1H), 2.41 (m, 2H), 2.23 (m, 3H), 1.96 (m, 2H), 1.62 (m, 3H), 1.90 (m, 1H), 1.09 (s, 3H), 0.89 (s, 9H), 0.04 (s, 6H) ppm; ¹³C NMR (CDCl₃, 75 MHz) δ 213.4, 79.8, 43.5, 43.4, 42.3, 36.8, 32.3, 32.1, 28.3, 25.7, 20.3, 18.0, –4.5, –4.9 ppm; mass (EI) m/z 282 (0.9%, M⁺), 267 (3.8%), 225 (100%). HREIMS m/z , found for C₁₆H₃₀O₂Si: 282.2053.

Preparation of the A-Ring Components. The Protected 4-Bromophenols. These compounds were prepared from the commercially available 4-bromophenols by reaction with either TBDMS chloride or MOM-Cl in CH₂Cl₂ in the presence of triethylamine, catalyzed by DMAP. Bromophenols that were not available commercially were prepared by standard bromination procedures starting either with the bromophenol itself or with the corresponding methoxyphenol followed by demethylation with PBr₃ in dichloromethane. The appropriate 4-bromophenol (25 mmol) and imidazole (1.25 equiv) were dissolved in a 1:1 DMF/THF solution (15 mL). TBDMSCl (1.25 equiv) and DMAP (trace) were added, and the reaction mixture was stirred overnight at room temperature. The mixture was diluted with distilled water (75 mL) and ether (75 mL)

and then extracted with ethyl acetate (3×75 mL). The organic extracts were combined, dried over MgSO_4 , filtered, and evaporated in vacuo. The crude product was purified on a flash column. Elution with hexane afforded the desired product as a clear colorless oil in generally greater than 90% yield. All compounds produced by this route had ^1H and ^{13}C NMR spectra in agreement with the desired structures.

Protection of the Bromophenols as MOM Ethers. *N,N*-Diisopropylethylamine (49.7 mmol) and chloromethyl methyl ether (49.7 mmol) were added to a solution of 4-bromophenol (24.9 mmol) in 30 mL of dry dichloromethane (DCM) under nitrogen atmosphere at 0°C . The resulting yellow mixture was stirred for 30 min at 0°C and then left overnight at room temperature. The organic mixture was diluted with aqueous 10% NaOH (30 mL) and extracted with dichloromethane (3×30 mL). The organic layers were combined, dried over MgSO_4 , filtered, and concentrated in vacuo. The crude product was purified on a silica column. Elution with 15% ethyl acetate in hexane afforded the desired product as a yellowish oil with yields approaching 97%. All compounds produced by this route had ^1H and ^{13}C NMR spectra in agreement with the desired structures.

Coupling of the Protected 4-Bromophenols [Ring A] with the Unprotected Hajos–Parrish Ketone. Protected bromophenol derivative (8.92 mmol) was dissolved in dry THF (20 mL) under nitrogen. The solution was placed in a dry ice/acetone bath (-78°C), and *n*-butyllithium (8.92 mmol) was added dropwise. The solution was stirred for 5 min, and a solution of unprotected Hajos–Parrish ketone (2.97 mmol), dissolved in dry THF (2 mL), was added dropwise. The reaction mixture was quenched after 10 min with saturated NH_4Cl solution (10 mL) and water (10 mL). The solution was extracted with EtOAc (3×30 mL), dried over MgSO_4 , filtered, and evaporated under vacuo. Flash chromatography of the crude product starting the elution with 30% EtOAc/hexane to 50% EtOAc/hexane generally allowed the clean separation of both stereoisomers with overall yields approaching 80%. The isomers having the A ring in the equatorial position relative to the CD ring eluted first. All compounds produced by this route had ^1H and ^{13}C NMR spectra in agreement with the desired structures.

Coupling of the Protected 4-Bromophenols [Ring A] with O-Protected Hajos–Parrish Ketone. Suitably protected bromophenol (2.94 mmol) was dissolved in dry THF (20 mL) and placed in a dry ice/acetone bath (-78°C). *n*-Butyllithium (2.94 mmol) was added dropwise, and the solution was left to stir for 5 min. A protected CD ring (1.67 mmol) was dissolved in dry THF (2 mL) and added dropwise. After 10 min, the reaction mixture was quenched with saturated NH_4Cl solution (10 mL) and water (10 mL). The solution was extracted with EtOAc (3×30 mL), dried over MgSO_4 , filtered, and evaporated under vacuo. The crude product was eluted with 5% EtOAc/hexane to 10% EtOAc/hexane on a silica gel column, affording a mixture of both isomers, typically in 75% yield. All compounds produced by this route had ^1H and ^{13}C NMR spectra in agreement with the desired structures.

Preparation of the Mixture of C Ring Unsaturated Compounds. Either the mixture of isomers obtained in the coupling reaction or the purified individual isomers can be used. A mixture of both isomers (0.146 mmol) of the condensation products of A and CD rings obtained using one of the two general procedures A and B described above was dissolved in toluene (2 mL). A trace of *p*-toluenesulfonic acid (PTSA) was added. The solution was kept at room temperature until TLC showed the disappearance of the starting material. The mixture was concentrated in vacuo and subjected to silica gel column chromatography. Elution with 20% ethyl acetate/80% hexane afforded a mixture of both isomers usually in more than 85% yield.

Dehydration and Deprotection of the TBDMS-Protected Phenols. The compounds were dehydrated by treatment with a catalytic amount of TsOH in either toluene or CH_2Cl_2 at room temperature. The progress of the reaction was followed by TLC. A mixture of the C9–C8 and C-9–C11 compounds was always

obtained; the yield of product was essentially quantitative. The TBDMS group was removed upon treatment with TBAF in THF at room temperature to yield a mixture of the C9–C8 and C9–C11 unsaturated diols.

The above dehydration mixture (0.130 mmol) was dissolved in THF (3 mL), and TBAF (0.130 mmol) was added to the solution dropwise. The resulting mixture was left for 10 min, diluted with brine (1 mL) and water (1 mL), and extracted with EtOAc (3×10 mL). The organic layers were combined, dried over MgSO_4 , filtered, and concentrated in vacuo. The crude product was subjected to a silica gel column chromatography. Elution with 25% EtOAc/75% hexane afforded the product mixture, generally in greater than 80% yield. All compounds produced by this route had ^1H and ^{13}C NMR spectra in agreement with the desired structures.

Dehydration and Deprotection of the Isomeric 9-Hydroxy-di-MOM Protected A-CD Adducts. The mixture of adducts was refluxed in methanol containing a catalytic amount of TsOH . The progress of the reaction was monitored by TLC. At the end most of the methanol was evaporated, ethyl acetate was added, and the mixture was washed with 5% NaHCO_3 . Evaporation of the organic solvents after drying over MgSO_4 afforded a mixture of the C9–C8 and C9–C11 unsaturated 3-17-diols. Separation of these isomers was accomplished using JAI Prep-Recycling HPLC.

Deprotection of the 9-Hydroxy-di-TBDMS A-CD Adducts To Form the 3,9,17-A-CD Triols. This reaction was carried out at room temperature with 1.3 equiv of TBAF in THF. The reaction progress was monitored by TLC; the typical reaction time was less than 15 min. The mixture was then diluted with brine and extracted with ethyl acetate. The organic layer was dried and the solvent evaporated to yield the mixture of isomers [3, 9-(*S*), 17-(*S*) and 3, 9-(*R*), 17-(*S*)] triols. These were separated on silica gel chromatography or HPLC.

Hydrogenation of the C-Ring Unsaturated Derivatives. The hydrogenations were carried out at room temperature in methanol with Pd/C and hydrogen under balloon pressure. In the same cases, such as with the 5- CF_3 compounds, the hydrogenation was carried out under X atm of hydrogen pressure. The products were isolated by filtering off the catalyst and evaporating the solvent. The yield of an approximately 1:1 mixture of 9-(*S*) and 9-(*R*) diastereomers was typically greater than 90%. The isomers were separated by either silica gel or preparative HPLC.

Hydrogenation of the 3-TBDMS or 3,17-di-TBDMS protected C-ring unsaturated isomers was carried out in a similar manner. The BDMS protecting groups were then removed as described above to yield again an approximately 1:1 mixture of 9-(*S*) and 9-(*R*) diastereomers.

Hydrogenolysis of the 9-OH-3,17-di-MOM Adducts. The mixture of adducts was dissolved in dichloromethane at -78°C and reacted with 3 equiv of triethylsilane. The reaction mixture was stirred at low temperature for 30 min, allowed to warm to room temperature, and then quenched with NH_4Cl solution. The organic layer was separated, dried, and the solvent was removed. The mixture of the 9-(*S*) and 9-(*R*) isomers thus obtained was separated into the two isomers by preparative HPLC.

Preparation of the 17-Ethynyl A-CD. To a solution of saturated final compound (0.2 mmol) in acetone (5 mL) was added Jones' reagent (0.22 mmol). The mixture was stirred at room temperature for 5 min. Isopropanol (0.5 mL) was added. Solvent was evaporated under vacuo and extracted with EtOAc (3×5 mL). The organic layers were combined, dried over MgSO_4 , and evaporated under vacuo to give a white gummy oil. Purification of crude product by flash chromatography afforded a white solid with 90% yield.

A solution of the above oxidized product (1.0 mmol) in dry dimethylsulfoxide (10 mL) under nitrogen was treated with lithium acetylide–ethylenediamine complex (300 mg), and the mixture was stirred at room temperature for 16–20 h. The mixture was poured into cold water, acidified with dilute acetic acid, extracted with ethyl acetate, washed with water and brine, and dried over MgSO_4 . After evaporation of the solvent under reduced pressure, the residue was chromatographed on silica gel

with 10–20% ethyl acetate in hexane to yield the desired compound.

Spectroscopic [^1H and ^{13}C NMR] and HRMS Data. 1a. ^1H NMR (400 MHz, acetone- d_6) δ 1.35 (s, 3H), 1.24 (m, 1H), 1.30 (m, 1H), 1.65 (m, 5H), 1.80 (m, 2H), 2.09 (m, 1H), 2.21 (m, 1H), 2.65 (m, 1H), 3.67 (brs, 1H), 6.76 (d, J = 8.5 Hz, 2H), 7.07 (d, J = 8.5 Hz, 2H), 8.17 (OH); ^{13}C NMR (acetone- d_6 , 100 MHz) δ 19.9, 28.2, 31.4, 33.7, 34.0, 34.2, 39.0, 43.3, 45.6, 83.2, 116.7, 129.4, 140.0, 157.1; mass (EI) m/z 246 (48.3%, M^+), 228 (2.5%), 202 (4.2%), 146 (10.9%), 120 (100%); HREIMS m/z calculated for $\text{C}_{16}\text{H}_{22}\text{O}_2$ 246.1779.

1b. ^1H NMR (400 MHz, acetone- d_6) δ 0.90 (3H, s), 1.12–1.39 (4H, m), 1.56–1.62 (4H, m), 1.72 (1H, quintet, J = 6.24 Hz), 1.92 (1H, dt, J = 13.73 and 3.09 Hz), 2.37–2.45 (1H, m), 3.44 (1H, d, J = 5.60 Hz), 4.36–4.41 (1H, m), 6.84–6.91 (2H, m), 6.94–6.97 (1H, m), 8.33 (1H, s); ^{13}C NMR (100 MHz, acetone- d_6) δ 24.0, 28.6, 34.9, 40.9, 44.4, 44.7, 46.9, 73.9, 115.7, 115.9, 119.3, 119.4, 124.4, 124.4, 141.8, 141.9, 152.0, 152.1. All of the aromatic carbons are recorded as two peaks due to coupling with F.

1c. ^1H NMR (400 MHz, acetone- d_6) δ 0.91 (3H, s), 1.13–1.20 (1H, m), 1.25–1.32 (1H, m), 1.37 (1H, dd, J = 13.10 and 4.62 Hz), 1.53–1.68 (4H, m), 1.74 (1H, quintet, J = 6.20 Hz), 1.93 (1H, dt, J = 13.78 and 3.21 Hz), 2.09–2.15 (1H, m), 2.69 (1H, tt, J = 12.23 and 3.21 Hz), 2.89 (1H, s), 3.45 (1H, d, J = 5.04 Hz), 4.36–4.40 (1H, m), 6.52 (1H, dd, J = 12.26 and 2.46 Hz), 6.60 (1H, dd, J = 8.40 and 2.43 Hz), 7.10 (1H, t, J = 8.63 Hz), 8.49 (1H, s); ^{13}C NMR (100 MHz, acetone- d_6) δ 24.0, 28.6, 30.1, 34.9, 37.8, 37.9, 39.5, 44.4, 46.9, 73.9, 104.2, 104.5, 113.0, 113.1, 126.3, 126.5, 129.8, 129.9, 158.5, 158.6, 161.6, 164.0. All of the aromatic carbons are recorded as two peaks due to coupling with F.

1d. ^1H NMR (400 MHz, acetone- d_6) δ 0.91 (s, 3H), 1.96–1.12 (m, 18H), 3.48 (m, 1H), 4.38 (t, J = 8.0 Hz, 1H), 6.75 (dd, J = 8.4, 2.4 Hz, 1H), 6.84 (d, J = 2.4 Hz, 1H), 7.15 (d, J = 8.8 Hz, 1H); ^{13}C NMR (100 MHz, CDCl_3) δ 20.9, 27.2, 30.4, 33.4, 34.1, 34.6, 39.8, 42.1, 44.5, 81.3, 114.1, 116.0, 124.7, 130.8, 134.0, 157.0.

1e. ^1H NMR (400 MHz, acetone- d_6) δ 1.14 (3H, s), 1.23–1.29 (1H, m), 1.36 (1H, td, J = 13.24 and 3.78 Hz), 1.48–1.54 (1H, m), 1.58–1.62 (3H, m), 1.64–1.71 (1H, m), 1.80–1.87 (2H, m), 2.23 (3H, s), 2.90 (3H, s), 3.42 (1H, d, J = 4.25 Hz), 3.65 (1H, t, J = 4.74 Hz), 6.61–6.64 (2H, m), 7.08 (1H, d, J = 8.34 Hz), 7.93 (1H, s); ^{13}C NMR (100 MHz, acetone- d_6) δ 20.2, 20.4, 28.4, 33.9, 34.0, 34.6, 34.8, 43.7, 45.9, 83.3, 114.7, 118.8, 128.1, 138.0, 138.0, 156.8.

1f. ^1H NMR (400 MHz, CDCl_3) δ 1.16 (s, 3H), 1.31–1.25 (m, 4H), 1.75–1.56 (m, 4H), 1.92–1.75 (m, 2H), 2.13–2.07 (m, 1H), 2.35–3.33 (m, 1H), 3.12–3.02 (m, 1H), 3.74 (d, J = 5.6 Hz, 5.30 (m, 1H), 6.97 (dd, J = 8.4, 2.4 Hz, 1H), 7.07 (d, J = 2.8 Hz, 1H), 7.35 (d, J = 8.8 Hz, 1H); ^{13}C NMR (100 MHz, CDCl_3) δ 18.4, 26.2, 29.3, 29.7, 32.1, 32.5, 33.1, 33.1, 41.5, 44.0, 82.6, 112.7, 118.7, 129.4, 138.3, 138.3, 153.3.

1g. ^1H NMR (400 MHz, CDCl_3) δ 1.10 (3H, s), 1.24–1.28 (3H, m), 1.46–1.57 (2H, m), 1.69–1.77 (2H, m), 1.82–1.91 (1H, m), 2.06–2.13 (1H, m), 2.18–2.27 (1H, m), 2.61 (1H, tt, J = 12.38 and 3.69 Hz), 3.73 (1H, d, J = 5.84 Hz), 5.22 (1H, s), 6.76 (2H, d, J = 9.00 Hz); ^{13}C NMR (100 MHz, CDCl_3) δ 18.3, 26.5, 29.2, 31.7, 32.0, 31.2, 37.4, 41.3, 44.0, 82.4, 109.7, 109.8, 109.8, 109.9, 110.0, 130.6, 139.5, 150.4, 150.4, 152.8. Additional “aromatic peaks” are recorded due to coupling to the F atoms on the ring.

1h. ^1H NMR (400 MHz, CDCl_3) δ 1.12 (3H, s), 1.25–1.29 (3H, m), 1.61–1.67 (3H, m), 1.70–1.77 (2H, m), 1.83–1.92 (1H, m), 2.08–2.14 (1H, m), 2.19–2.28 (1H, m), 2.62 (1H, tt, J = 12.31 and 3.82 Hz), 3.73 (1H, d, J = 5.78 Hz), 5.73 (1H, s), 7.12 (2H, s); ^{13}C NMR (100 MHz, CDCl_3) δ 22.1, 26.8, 29.3, 29.9, 32.8, 38.6, 42.6, 42.8, 44.9, 73.6, 109.5, 109.6, 109.7, 109.8, 109.8, 130.5, 139.5, 152.7, 152.8.

1i. ^1H NMR (400 MHz, acetone- d_6) δ 1.12 (3H, s), 1.22–1.28 (1H, m), 1.35 (1H, td, J = 13.24 and 3.90 Hz), 1.54–1.62 (2H, m), 1.64–1.74 (3H, m), 1.76–1.84 (2H, m), 2.08–2.13 (1H, m), 2.18–2.27 (1H, m), 3.01 (2H, tt, J = 12.35 and 3.84 Hz), 3.65 (1H, d, J = 5.66 Hz), 6.76 (1H, td, J = 8.42 and 1.96 Hz), 6.95 (1H, td, J = 8.19 and 2.26 Hz); ^{13}C NMR (100 MHz, acetone- d_6) δ 20.0, 28.2, 29.9,

32.7, 32.8, 33.9, 34.0, 43.3, 45.8, 83.2, 114.4, 114.4, 123.2, 123.2, 123.2, 123.3, 128.1, 128.1, 128.2, 128.3, 140.8, 143.2, 143.4, 146.0, 146.1, 146.1, 146.2, 150.0, 152.4. Additional “aromatic peaks” are recorded due to coupling to the F atoms on the ring.

1j. ^1H NMR (400 MHz, CDCl_3) δ 1.25 (s, 3H), 1.86–1.34 (m, 10H), 2.35–1.99 (m, 4H), 2.74–2.61 (m, 1H), 3.00–2.90 (m, 1H), 4.23 (d, J = 7.6 Hz, 1H), 5.18 (m, 1H), 6.69 (dd, J = 14.0, 9.6 Hz, 1H), 6.94 (dd, J = 15.2, 8.8 Hz, 1H).

1k. ^1H NMR (400 MHz, acetone- d_6) δ 1.14 (3H, s), 1.33 (2H, m), 1.69 (4H, m), 1.85 (2H, m), 2.10 (1H, m), 2.26 (1H, m), 3.03 (1H, m), 3.66 (1H, d, J = 5.66 Hz), 6.85 (1H, m); ^{13}C NMR (100 MHz, CDCl_3) δ 19.9, 28.17, 29.65, 32.60, 33.80, 33.86, 43.22, 45.77, 83.15, 110.10, 109.89, 127.15, 127.08, 134.72, 134.67, 141.90, 141.80, 144.32, 144.15, 146.13, 146.27, 148.54, 148.65, 149.05, 149.06, 151.41.

1l. ^1H NMR (400 MHz, CDCl_3) δ 1.13 (s, 3H), 1.58 (s, 3H), 1.65–1.60 (m, 2H), 1.71–1.67 (m, 2H), 1.92–1.75 (m, 2H), 2.15–2.07 (m, 1H), 2.15 (d, J = 2 Hz, 3H), 2.31–2.22 (m, 1H), 3.02–2.94 (m, 1H), 3.73 (d, J = 5.6 Hz, 1H), 4.77 (m, 1H), 6.53 (d, J = 8.4 Hz, 1H), 6.94 (t, J = 8.4 Hz, 1H), 6.97 (dd, J = 8.4, 2.4 Hz, 1H); ^{13}C NMR (100 MHz, CDCl_3) δ 18.7, 26.5, 29.6, 32.4, 32.4, 32.8, 41.8, 44.3, 77.6, 82.94, 113.0, 113.0, 119.1, 129.8, 153.6.

1o. ^1H NMR (400 MHz, CDCl_3) δ 1.14 (s, 3H), 1.31 (dd, J = 3.6, 8.4 Hz, 2H), 1.42–1.36 (m, 1H), 1.70–1.54 (m, 6H), 1.96–1.78 (m, 2H), 2.15–2.08 (m, 1H), 2.19 (s, 3H), 2.22 (s, 3H), 2.15–2.07 (m, 1H), 2.32–2.25 (m, 1H), 2.31–2.22 (m, 1H), 2.92 (tt, J = 4, 12 Hz, 1H), 3.74 (d, J = 5.6 Hz, 1H), 4.61 (m, 1H), 6.63 (d, J = 8.0 Hz, 1H), 7.00 (d, J = 8.4 Hz, 1H); ^{13}C NMR (100 MHz, CDCl_3) δ 12.22, 14.97, 18.47, 26.54, 28.50, 31.93, 32.09, 32.59, 33.66, 41.76, 44.27, 82.62, 112.33, 122.61, 123.34, 135.57, 137.43, 151.37.

Compound 2. ^1H NMR (400 MHz, acetone- d_6) δ 1.11 (s, 3H), 1.17 (m, 1H), 1.59 (m, 3H), 1.82 (m, 3H), 2.12 (m, 3H), 2.43 (m, 1H), 2.74 (m, 1H), 6.76 (d, J = 8.5 Hz, 2H), 7.10 (d, J = 8.5 Hz, 2H), 8.08 (OH) ppm; ^{13}C NMR (100 MHz, acetone- d_6) δ 20.2, 24.6, 30.4, 34.5, 37.5, 39.0, 45.0, 47.9, 116.9, 129.5, 139.6, 157.4, 207.1.

Compound 3. ^1H NMR (400 MHz, acetone- d_6) δ 1.21 (s, 3H), 1.40–1.80 (m, 10H), 2.04 (m, 1H), 2.64 (m, 1H), 6.74 (d, J = 8.4 Hz, 2H), 7.08 (d, J = 8.4 Hz, 2H); ^{13}C NMR (acetone- d_6 , 100 MHz) δ 18.8, 23.1, 28.3, 29.8, 33.2, 37.3, 37.6, 42.1, 73.0, 80.4, 88.3, 115.0, 127.7, 138.2, 155.4.

Compound 4. ^1H NMR (400 MHz, acetone- d_6) δ 1.02 (s, 3H), 1.44–1.29 (m, 2H), 1.65–1.57 (m, 2H), 2.33–2.02 (m, 7H), 3.88 (t, J = 6.0 Hz, 1H), 5.55 (m, 1H), 6.74 (dd, J = 8.4, 2.4 Hz, 1H), 6.85 (d, J = 2.4 Hz, 1H), 7.02 (d, J = 8.4 Hz, 1H); ^{13}C NMR (400 MHz, acetone- d_6) δ 19.4, 26.3, 28.4, 28.6, 28.7, 28.8, 29.0, 29.2, 29.4, 29.5, 29.7, 30.2, 31.9, 42.2, 44.1, 77.5, 114.1, 115.9, 130.8, 131.0, 132.3, 134.3, 134.8, 156.8.

Compound 5. ^1H NMR (400 MHz, acetone- d_6) δ 1.07 (s, 3H), 1.56–1.44 (m, 2H), 1.75–1.69 (m, 1H), 1.84–1.77 (m, 1H), 1.88 (dq, 1H), 2.23–2.03 (m, 5H), 2.39 (m, 1H), 3.75 (dd, J = 6.0, 1.6 Hz, 1H), 5.50 (m, 1H), 6.74 (dd, J = 8.4, 2.4 Hz, 1H), 6.84 (d, J = 2.4 Hz, 1H), 7.01 (d, J = 8.4 Hz, 1H); ^{13}C NMR (acetone- d_6 , 100 MHz) δ 19.8, 28.0, 28.4, 28.6, 28.8, 29.0, 29.2, 29.3, 29.4, 29.6, 29.7, 31.8, 32.2, 39.8, 42.1, 79.3, 114.1, 116.0, 124.7, 130.8, 132.3, 134.0, 135.0, 157.0.

Force Field Calculations. For calculations involving rotational potential energy barriers resulting from twisting about the A–C bond and for all docking calculations, we used the MMFF94s force field as implemented in the MOE software (Molecular Operating Environment 2009, Chemical Computing Group, Montreal, Canada). This force field is parametrized for use in medicinal chemistry. A distance-dependent dielectric constant was used (from 1 to 80) with a cutoff at 10 Å.

Docking and Scoring. X-ray crystallographic data for human recombinant ER α and ER β were obtained from the RCSB database. All programs described here are available free of charge from www.shadnia.com. Of the four existing crystal structures of E2 with ER α (1GWR, 1G50, 1ERE, 1A52) and the two existing crystal structures of the selective ligand genistein with ER β (1QKM,

1X7R) we used those with the better resolution (1GWR for ER α) or the one containing the E2 ligand (2J7X for ER β). Hydrogen atoms were added and partial charges assigned to charged residues at pH 7. To energy-minimize the complex, we used our H_PDB-Thaw program. The program uses artificial force constants to simulate gradients of flexibility during energy minimization cycles. Initially, the ligand and active site atoms are kept very rigid, and their rigidity is gradually reduced as energy minimization progresses. At the final step all atoms are flexible and energy minimization is performed in the normal fashion. The algorithm minimizes the movement of active site atoms due to energy minimization, keeping the active site as close as possible to the original crystal coordinates.

The docking procedure was performed using our uDock program, which runs under the MOE software environment. To accelerate the calculations, a "shell" model of the active site was generated from the full protein. All residues having at least one atom closer than 6 Å to the cocrystallized reference ligand were selected as the inner shell S1. The second shell, S2, was defined as all atoms of all amino acids having at least one atom closer than 4.5 Å to the S1 atoms, excluding those already defined in S1. The rest of the atoms were deleted and the broken bonds were capped with hydrogen atoms, making the third shell S3. Thus, for E2 in ER α , S1 included all the active site atoms, containing 45 residues (664 atoms), S2 included 84 residues (1295 atoms), and S3 contained 25 atoms. During the docking, S3 was fixed, S2 was tethered (tether constant of 30), and S1 (active site) was flexible. Instead of computing the entire complex energy, only energies of ligand + S1 were used, and the rest of the atoms were excluded from energy calculations, including the cofactor peptide. A more complete description of the procedures used in uDock and PDB_Thaw is included in the Supporting Information.

The cofactor binding is known to stabilize the closed conformation of the ligand–receptor complex. It is also known that in the case of antagonist or mixed agonist ligands with an extra bulky group, a displacement of the cofactor-binding helix (H12) is required to allow the active site changes necessary to accommodate such ligands. However, in the case of agonist ligands that are smaller than E2, the cofactor binding has no direct effect on the active site. This can be demonstrated by superposition of experimental data; for example, the active sites of the three complexes of ER α with E2 (PDB entries 1GWR, 1ERE, 1G50) show a heavy atom rmsd of only 0.3 Å, and the only visible difference is rotation of the methionone *S*-methyl groups which has a low energy barrier and can even be seen in comparison of the two monomer proteins from the same PDB entry (for example, the chain A, B from the PDB entry 1GWR). Thus, we think deleting the exterior parts of the receptor and the cofactor peptide has no significant effect on the docking.

Next, a database of ligand conformers was generated using the systematic conformer search utility in MOE. Rotatable bonds were incremented in 20° steps and energy-minimized, and redundant structures were removed. All final conformers within 7 kcal/mol of the lowest-energy conformer were retained for docking.

To generate initial poses, the ligand conformers were randomly placed inside a virtual box called the docking box, defined with a margin of 1 Å from the receptor cavity (defined by the van der Waals surface of the active site). The initial complex was then energy-minimized, while the junction shell atoms are fixed but the active shell atoms are fully flexible. A docking job was considered to be converged when at least five of the top-ranked complexes for each ligand were similar (difference in force field energies of < 1 kcal/mol). The energy-minimized poses should be ranked by the energy of the entire complex. Since we used the truncated model of the protein, the energy of the flexible shell plus ligand was used as a substitute for the energy of the entire protein. Solvation energies of the ligand were calculated using CPCM method in Gaussian 03 on AM1 optimized global minimum energy geometries of the ligand (keywords: HF/6-31G(d), SCRF = (CPCM,Read,Solvent = Water)). A scoring function was developed on the basis of parameters defining each

ligand–receptor complex and used to create multiple linear regression models to be correlated with the experimental RBAs.

The volume calculations were performed using our H_CavityGridVol program. The program renders the van der Waals surface of the active site and then counts the number of points in a 3D grid (0.25 Å steps) that fall within the cavity boundary. The interaction energies were calculated and graphed using our H_INTERACT and H_GIE programs.

BDE Calculation. Bond dissociation enthalpies (BDEs) for the phenolic OH bond were calculated using the MLM2 method,⁵⁸ a variant of density functional theory (DFT) that uses the B3LYP functional as implemented in the Gaussian 03 software package (Gaussian, Inc.) and has been shown to be accurate to within ± 1 kcal/mol for a variety of substituted phenols.^{58,59} Briefly, the medium-level model 2 (MLM2) method calculates geometries and frequencies using the B3LYP/6-31G(d) method/basis set and scales frequencies by the factor 0.9805. For the parent phenol the electronic energy is obtained using B3LYP/6-311+G(2d,2p) at the smaller basis potential minimum. The same procedure is used for the phenoxyl radical except that the restricted open shell functional ROB3LYP is used to obtain the large-basis energy at the B3LYP/6-31G(d) potential minimum. The electronic energy of the H-atom is set to its exact value of -0.50000 au (1 au = 627.51 kcal/mol), giving an enthalpy value ($E_{\text{electronic}} + \frac{5}{2}RT$) = -0.49764 au at 298.15 K. The BDE for formation of the phenoxyl radical is given by $\text{BDE} = \Delta H_{\text{rxn}} = H_{\text{phenoxyl}} + H_{\text{H}} - H_{\text{phenol}}$, where the absolute enthalpies H contain the thermal correction to the enthalpy at 298.15 K.

Binding Affinity Assays. Relative binding affinities (RBAs) to the estrogen receptors ER α and ER β were determined by a competitive radiometric binding assay as previously described^{30,32} using 10 nM [³H]estradiol as tracer. Purified full-length human ER α and ER β were purchased from PanVera (Madison, WI, U.S.). Incubations were done for 18–24 h at 0 °C. Hydroxyapatite (Bio-Rad, Hercules, CA) was used to absorb the ligand–receptor complexes, and free ligand was washed away. Binding affinities are expressed relative to the binding affinity of E2, which is set to 100%. E2 binds to ER α with a K_d of 0.2 nM and to ER β with a K_d of 0.5 nM.

Gene Transcription Assays. HEK-293 cells were grown in phenol red-free (PRF) DMEM media (+Na pyruvate, +10% charcoal-treated stripped FBS). Cells were plated into six-well plates at 2 mL/well at a cell density of 1.2×10^5 cells per well. Cells were immediately transfected with polyethylenimine (PEI), serum-free DMEM, and optimal amounts (1 μ g each) of the ER α or ER β expression vector plus the estrogen response element (ERE) luciferase reporter gene. The cells were incubated for 24 h at 37 °C, after which ligand was added. E2 was used as control and EtOH as vehicle (blank). The transfected HEK293 cells were treated with 2 μ L of each ligand (1:1000 dilution in EtOH) for a final concentration of 10 nM. After 48 h of incubation at 37 °C the cells were lysed by removing the media, washing twice with PBS, and then adding 85 μ L of lysis buffer. After 15 min at room temperature, 20 μ L of lysate was combined with 100 μ L of luciferase assay buffer and immediately placed in a Lumat LB9507 (Berthold Technology) luminometer for measurement of light intensity. Each ligand dose was performed in triplicate. Relative error was computed as the standard error of the three values from the mean. All experiments were repeated at least three times with similar results.

Hepatotoxicity Assay. Adult male Sprague–Dawley rats, 250–300 g, were obtained from Charles River Canada Laboratories (Montreal, Canada), fed ad libitum, and allowed to acclimatize for 1 week. All animal treatment conformed to guidelines provided by the University of Toronto, Canada. Hepatocytes were isolated from rats by collagenase perfusion of the liver as described by Moldeus et al.⁷² An amount of 10 mL of isolated hepatocytes (10^6 cells/mL) was suspended in Krebs–Henseleit buffer (pH 7.4) containing 12.5 mM HEPES in continually rotating round-bottomed flasks under an atmosphere of 95% O₂ and 5% CO₂ in a water bath (37 °C) for 30 min. Stock solutions of the test compounds prepared

in ethanol were added to the solution containing the hepatocytes to achieve the desired concentrations and incubated under the oxygen-rich atmosphere described above. The lethal concentration that killed 50% of the cells (LC_{50}) after incubation for 2 h was determined by counting the number of cells that excluded trypan blue (0.1% w/v). All measurements were done in triplicate to obtain the stated ranges (Table 2).

Acknowledgment. We thank the Canadian Breast Cancer Foundation (Ontario region) for grants to J.S.W. and T.D. in support of this work. Some calculations have been performed on the High Performance Virtual Computing Laboratory (HPCVL.org) at Kingston, Ontario, Canada.

Supporting Information Available: uDock user manual. This material is available free of charge via the Internet at <http://pubs.acs.org>.

References

- (1) Writing Group for the Women's Health Initiative Investigators. Risks and benefits of estrogen plus progestin in healthy postmenopausal women: principal results from the Women's Health Initiative randomized controlled trial. *JAMA, J. Am. Med. Assoc.* **2002**, *288*, 321–323.
- (2) Chlebowski, R. T.; Hendrix, S. L.; Langer, R. D.; Stefanick, M. L.; Gass, M.; Lane, D.; Rodabough, R. J.; Gilligan, M. A.; Cyr, M. G.; Thomson, C. A.; Khandekar, J.; Petrovitch, H.; McTiernan, A. Influence of estrogen plus progestin on breast cancer and mammography in healthy postmenopausal women. *JAMA, J. Am. Med. Assoc.* **2003**, *289*, 3243–3253.
- (3) Bernstein, L. The risk of breast, endometrial and ovarian cancer in users of hormonal preparations. MiniReview. *Basic Clin. Pharmacol. Toxicol.* **2006**, *98*, 288–296.
- (4) Parkin, D. M.; Whelan, S. L.; Ferlay, J.; Raymond, L.; Young, J. *Cancer Incidence in Five Continents*; Oxford University Press: Oxford, U.K., 1997.
- (5) Ruggiero, R. J.; Likis, F. E. Estrogen: physiology, pharmacology, and formulations for replacement therapy. *J. Midwifery Women's Health* **2002**, *47*, 130–138.
- (6) Wathen, C. N.; Feig, D. S.; Feightner, J. W.; Abramson, B. L.; Cheung, A. M.; Canadian Task Force on Preventive Health Care. Hormone replacement therapy for the primary prevention of chronic diseases: recommendation statement from the Canadian Task Force on Preventive Health Care. *Can. Med. Assoc. J.* **2004**, *170*, 1535–1537.
- (7) Hersh, A. L.; Stefanick, M. L.; Stafford, R. S. National use of postmenopausal hormone therapy: annual trends and response to recent evidence. *JAMA, J. Am. Med. Assoc.* **2004**, *291*, 47–53.
- (8) Cavalieri, E.; Chakravarti, D.; Guttenplan, J.; Hart, E.; Ingle, J.; Jankowiak, R.; Muti, P.; Rogan, E.; Russo, J.; Santen, R.; Sutter, T. Catechol estrogen quinones as initiators of breast and other human cancers. *Biophys. Acta, Rev. Cancer* **2006**, *1766*, 63–78.
- (9) Sarabia, S. F.; Zhu, B. T.; Kurosawa, T.; Tohma, M.; Liehr, J. G. Mechanism of cytochrome P450-catalyzed aromatic hydroxylation of estrogens. *Chem. Res. Toxicol.* **1997**, *10*, 767–771.
- (10) Zhang, F.; Chen, Y.; Pisha, E.; Shen, I.; Xioong, Y.; van Breemen, R. B.; Bolton, J. L. The major metabolite of equilin, 4-hydroxy-equilin, autoxidizes to an *o*-quinone which isomerizes to the potent cytotoxin 4-hydroxyequilenin-*o*-quinone. *Chem. Res. Toxicol.* **1999**, *12*, 204–213.
- (11) Bolton, J. L. Quinoids, quinoid radicals, and phenoxyl radicals from estrogens and antiestrogens: role in carcinogenesis? *Toxicology* **2002**, *177*, 55–65.
- (12) Liu, X.; Yao, J.; Pisha, E.; Yang, Y.; Hua, Y.; van Breemen, R. B.; Bolton, J. L. Oxidative DNA damage induced by equine estrogen metabolites: role of estrogen receptor. *Chem. Res. Toxicol.* **2002**, *15*, 512–519.
- (13) Liu, X.; Zhang, F.; Liu, H.; Burdette, J. E.; Li, Y.; Cassia, R. O.; Pisha, M.; Yao, J.; van Breemen, R. B.; Swanson, S. M.; Bolton, J. L. Effect of halogenated substituents on the metabolism and estrogenic effects of the equine estrogen, equilenin. *Chem. Res. Toxicol.* **2003**, *16*, 741–749.
- (14) Yu, L.; Liu, H.; Li, W.; Zhang, F.; Luckie, C.; van Breemen, R. B.; Thatcher, G. R. J.; Bolton, J. L. Oxidation of raloxifene to potential toxic quinoids: formation of a di-quinone methide and *o*-quinones. *Chem. Res. Toxicol.* **2004**, *17*, 879–888.
- (15) Cavalieri, E. L.; Rogan, E. G.; Chakravarti, D. Initiation of cancer and other diseases by catechol ortho-quinones: a unifying mechanism. *Cell. Mol. Life Sci.* **2002**, *59*, 665–681.
- (16) Cavalieri, E.; Rogan, E.; Chakravarti, D. The role of endogenous catechol quinones in the initiation of cancer and neurodegenerative diseases. *Methods Enzymol.* **2004**, *382B* (Quinones and Quinone Enzymes), 293–319.
- (17) Zahid, M.; Kohli, E.; Saeed, M.; Rogan, E.; Cavalieri, E. The greater reactivity of estradiol-3,4-quinone vs. estradiol-2,3-quinone with DNA in the formation of depurinating adducts: implications for tumor-initiating activity. *Chem. Res. Toxicol.* **2006**, *19*, 164–172.
- (18) Liehr, J. G. Genotoxicity of the steroidal oestrogens oestrone and oestradiol: possible mechanism of uterine and mammary cancer development. *Hum. Reprod. Update* **2001**, *10*, 273–281.
- (19) Hussain, H. H.; Babic, G.; Durst, T.; Wright, J. S.; Fluoraru, M.; Chichirau, A.; Chepelev, L. L. Development of novel antioxidants: design, synthesis, and reactivity. *J. Org. Chem.* **2003**, *68*, 7023–7032.
- (20) Chichirau, A.; Fluoraru, M.; Chepelev, L. L.; Wright, J. S.; Willmore, William, G.; Durst, T.; Hussain, H. H.; Charron, M. Mechanism of cytotoxicity of catechols and a naphthalenediol in PC12-AC cells: the connection between extracellular autoxidation and molecular electronic structure. *Free Radical Biol. Med.* **2005**, *38*, 344–355.
- (21) Fluoraru, M.; Chichirau, A.; Chepelev, L. L.; Willmore, W. G.; Durst, T.; Charron, M.; Barclay, L. R. C.; Wright, J. S. Cytotoxicity and cytoprotective activity in naphthalenediols depends on their tendency to form naphthoquinones. *Free Radical Biol. Med.* **2005**, *39*, 1368–1377.
- (22) Fluoraru, M.; So, R.; Willmore, W. G.; Poulter, M. O.; Durst, T.; Charron, M.; Wright, J. S. Cytotoxicity and cytoprotective activity of naphthalenediols in rat cortical neurons. *Chem. Res. Toxicol.* **2006**, *19*, 1221–1227.
- (23) O'Brien, P. J. Molecular mechanisms of quinone cytotoxicity. *Chem.-Biol. Interact.* **1991**, *80*, 1–41.
- (24) Pezzella, A.; Lista, L.; Napolitano, A.; d'Ischia, M. Tyrosinase-catalyzed oxidation of 17 β estradiol: structure elucidation of the products formed beyond catechol estrogen quinones. *Chem. Res. Toxicol.* **2005**, *18*, 1413–1419.
- (25) Klaus, V.; Hartmann, T.; Gambini, G.; Graf, P.; Stahl, W.; Hartwig, A.; Klotz, L. A. 1,4-Naphthoquinones as inducers of oxidative damage and stress signaling in aCaT human keratinocytes. *Arch. Biochem. Biophys.* **2010**, *496*, 93–100.
- (26) Kuiper, G. G. J.; Carlsson, B.; Grandien, K.; Enmark, E.; Häggblad, J.; Nilsson, S.; Gustafsson, J. Comparison of the ligand binding specificity and transcript tissue distribution of estrogen receptors α and β . *Endocrinology* **1997**, *138*, 863–870.
- (27) Kuiper, G. G. J.; Lemmen, J. G.; Carlsson, B.; Corton, J. C.; Safe, S. H.; van der Saag, P. T.; van der Burg, B.; Gustafsson, J. Interaction of estrogenic chemicals and phytoestrogens with estrogen receptor β . *Endocrinology* **1998**, *139*, 4252–4263.
- (28) Dahlman-Wright, K.; Cavailles, V.; Fuqua, S. K.; Jordan, V. C.; Katzenellenbogen, J. A.; Korach, K. S.; Maggi, A.; Muramatsu, M.; Parker, M. G.; Gustafsson, J.-A. International Union of Pharmacology. LXIV. Estrogen receptors. *Pharmacol. Rev.* **2006**, *58*, 773–781.
- (29) Fink, B. E.; Mortenson, D. S.; Stauffer, S. R.; Aron, Z. D.; Katzenellenbogen, J. A. Novel structural templates for estrogen-receptor ligands and prospects for combinatorial synthesis of estrogens. *Chem. Biol.* **1999**, *6*, 205–219.
- (30) De Angelis, M. D.; Stossi, F.; Carlson, K. E.; Katzenellenbogen, B. S.; Katzenellenbogen, J. A. Indazole estrogens: highly selective ligands for the estrogen receptor β . *J. Med. Chem.* **2005**, *48*, 1132–1144.
- (31) Gilli, P.; Gilli, G.; Borea, P. A.; Varani, K.; Scatturin, A.; Dalpiaz, A. Binding thermodynamics as a tool to investigate the mechanisms of drug-receptor interactions: thermodynamics of cytoplasmic steroid/nuclear receptors in comparison with membrane receptors. *J. Med. Chem.* **2005**, *48*, 2026–2035.
- (32) Anstead, G. M.; Carlson, K. E.; Katzenellenbogen, J. A. The estradiol pharmacophore: ligand structure–estrogen receptor binding affinity relationships and a model for the receptor binding site. *Steroids* **1997**, *62*, 268–303.
- (33) Ekena, K.; Weis, K. E.; Katzenellenbogen, J. A.; Katzenellenbogen, B. S. Different residues of the human estrogen receptor are involved in the recognition of structurally diverse estrogens and antiestrogens. *J. Biol. Chem.* **1997**, *272*, 5069–5075.
- (34) Carlson, K. E.; Choi, I.; Gee, A.; Katzenellenbogen, B. S.; Katzenellenbogen, J. A. Altered ligand binding properties and enhanced stability of a constitutively active estrogen receptor: evidence that an open pocket conformation is required for ligand interaction. *Biochemistry* **1997**, *36*, 14897–14905.
- (35) De Angelis, M.; Stossi, F.; Carlson, K. A.; Katzenellenbogen, B. S.; Katzenellenbogen, J. A. Indazole estrogens: highly selective ligands for the estrogen receptor beta. *J. Med. Chem.* **2005**, *48*, 1132–1144.

- (36) Stauffer, S. R.; Coletta, C. J.; Tedesco, R.; Nishiguchi, G.; Carlson, K.; Sun, J.; Katzenellenbogen, B. S.; Katzenellenbogen, J. A. Pyrazole ligands: structure–affinity/activity relationships and estrogen receptor- α -selective agonists. *J. Med. Chem.* **2000**, *43*, 4934–4947.
- (37) Katzenellenbogen, B. S.; Montano, M. M.; Ediger, T. R.; Sun, J.; Ekena, K.; Lazennec, G.; Martini, P. G.; McInerney, E. M.; Delage-Mourroux, R.; Weis, K.; Katzenellenbogen, J. A. Estrogen receptors: selective ligands, partners, and distinctive pharmacology. *Recent Prog. Horm. Res.* **2000**, *55*, 163–193; discussion 194–195.
- (38) Sun, J.; Meyers, M. J.; Fink, B. E.; Rajendran, R.; Katzenellenbogen, J. A.; Katzenellenbogen, B. S. Novel ligands that function as selective estrogens or antiestrogens for estrogen receptor- α or estrogen receptor- β . *Endocrinology* **1999**, *140*, 800–804.
- (39) Tedesco, R.; Thomas, J. A.; Katzenellenbogen, B. S.; Katzenellenbogen, J. A. The estrogen receptor: a structure-based approach to the design of new specific hormone-receptor combinations. *Chem. Biol.* **2001**, *8*, 277–287.
- (40) Sun, J.; Huang, Y. R.; Harrington, W. R.; Sheng, S.; Katzenellenbogen, J. A.; Katzenellenbogen, B. S. Antagonists selective for estrogen receptor α . *Endocrinology* **2002**, *143*, 941–947.
- (41) Asim, M.; El-Safiti, M.; Qian, Y.; Choueiri, C.; Salari, S.; Cheng, J.; Shadnia, H.; Bal, M.; Pratt, M. A. C.; Carlson, K. E.; Katzenellenbogen, J. A.; Wright, J. S.; Durst, T. Deconstructing estradiol: removal of B-ring generates compounds which are potent and subtype-selective estrogen receptor agonists. *Bioorg. Med. Chem. Lett.* **2009**, *19*, 1250–1253. Asim, M.; El-Safiti, M.; Qian, Y.; Choueiri, C.; Salari, S.; Cheng, J.; Shadnia, H.; Bal, M.; Pratt, M. A. C.; Carlson, K. E.; Katzenellenbogen, J. A.; Wright, J. S.; Durst, T. Deconstructing estradiol: removal of B-ring generates compounds which are potent and subtype-selective estrogen receptor agonists. *Bioorg. Med. Chem. Lett.* **2009**, *19*, 2605 (Erratum to document cited in CA150:423383).
- (42) Novello, F. C. 8-Methyl-5-(hydroxyphenyl)hexahydroindan compounds. US 2886589 19590512 CAN 53:111713 AN 1959:111713 CAPLUS, 1959.
- (43) Bindra, J. S.; Neyyarapally, A. T.; Gupta, R. C.; Kamboj, V. P.; Anand, N. Studies in antifertility agents. 8. Seco steroids. 2. 5,6-Secoestradiol and some related compounds. *J. Med. Chem.* **1975**, *18*, 921–925.
- (44) Neyyarapally, A. T.; Gupta, R. C.; Srivastava, S. C.; Bindra, J. S.; Groveer, P. K.; Setty, B. S.; Anand, N. Antifertility agents. Synthesis of dialkylaminoethoxy derivatives of 3-alkyl-2,3-diphenylpropionophenones. *Indian J. Chem.* **1973**, *11*, 325–329.
- (45) Suwandi, L. S.; Agoston, G. E.; Shah, J. H.; Hanson, A. D.; Zhan, X. H.; LaVallee, T. M.; Treston, A. M. Synthesis and antitumor activities of 3-modified 2-methoxyestradiol analogs. *Bioorg. Med. Chem. Lett.* **2009**, *19*, 6459–6462.
- (46) Agoston, G. E.; Shah, J. H.; Suwandi, L.; Hanson, A. D.; Zhan, X.; LaVallee, T. M.; Pribluda, V.; Treston, A. M. Synthesis, antiproliferative, and pharmacokinetic properties of 3- and 17-double-modified analogs of 2-methoxyestradiol. *Bioorg. Med. Chem. Lett.* **2009**, *19*, 6241–6244.
- (47) Shah, J. H.; Agoston, G. E.; Suwandi, L.; Hunsucker, K.; Pribluda, V.; Zhan, X. H.; Swartz, G. M.; LaVallee, T. M.; Treston, A. M. Synthesis of 2- and 17-substituted estrone analogs and their antiproliferative structure–activity relationships compared to 2-methoxyestradiol. *Bioorg. Med. Chem.* **2009**, *17*, 7344–7352.
- (48) Agoston, G. E.; Shah, J. H.; Hunsucker, K. A.; Treston, A. M.; Pribluda, V. S. Nonsteroidal Analogs of 2-Methoxyestradiol for the Treatment of Diseases Characterized by Undesirable Angiogenesis, Proliferative Activity, or Cell Mitosis. PCT Int. Appl. PCT/US2003/002728, 2003.
- (49) Agoston, G. E.; Shah, J. H.; Hunsucker, K. A.; Treston, A. M.; Pribluda, V. S. Nonsteroidal Analogs of 2-Methoxyestradiol for Treatment of Diseases Characterized by Undesirable Angiogenesis and Proliferative Activity. PCT Int. Appl. PCT/US2003/002917, 2003.
- (50) There is no specific reference for this statement, but it is an assumption that has been shared by many workers in the field of estrogen modeling because of the subnanomolar binding affinity of estradiol for ER α (J. A. Katzenellenbogen, personal communication).
- (51) Harris, H. A.; Katzenellenbogen, J. A.; Katzenellenbogen, B. S. Characterization of the biological roles of the estrogen receptors, ER α and ER β , in estrogen target tissues in vivo through the use of an ER α -selective ligand. *Endocrinology* **2002**, *143*, 4172–4177.
- (52) Ghosh, U.; Ganessunker, D.; Sattigeri, V. J.; Carlson, K. E.; Mortensen, D. J.; Katzenellenbogen, B. S.; Katzenellenbogen, J. A. Estrogenic diazenes: heterocyclic non-steroidal estrogens of unusual structure with selectivity for estrogen receptor subtypes. *Bioorg. Med. Chem.* **2003**, *11*, 629–657.
- (53) An erratum containing this correction was sent to the editor of *BioOrganic and Medicinal Chemistry Letters* in August, 2010.
- (54) Micheli, R. A.; Hajos, Z. G.; Cohen, N.; Parrish, D. R.; Portland, L. A.; Sciamanna, W.; Scott, M. A.; Wehrli, P. A. Total syntheses of optically active 19-nor steroids. (+)-Estr-4-ene-3,17-dione and (+)-13 β -ethylgon-4-ene-3,17-dione. *J. Org. Chem.* **1975**, *40*, 675–681.
- (55) Hajos, Z. G.; Parrish, D. R. (+)-(7aS)-2,3,7,7a-Tetrahydro-7a-methyl-1H-indene-1,5-(6H)-dione (1H-indene-1,5(6H)-dione, 2,3,7,7a-tetrahydro-7a-methyl-, (S)-). *Org. Synth.* **1985**, *63*, 26–36.
- (56) Ward, D. E.; Rhee, C. K.; Zoghaib, W. M. A general method for the reductive reduction of ketones in the presence of enones. *Tetrahedron Lett.* **1988**, *29*, 517–520.
- (57) Wayner, D. D. M.; Luszyk, E.; Page, D.; Ingold, K. U.; Mulder, P.; Larhoven, L. J. J.; Aldrich, H. S. Effects of solvation on the enthalpies of reaction of *tert*-butoxyl radicals with phenol and on the calculated O–H bond strength in phenol. *J. Am. Chem. Soc.* **1995**, *117*, 8737–8744.
- (58) DiLabio, G. A.; Pratt, D. A.; LoFaro, A. D.; Wright, J. S. Theoretical study of X–H bond energetics (X = C, N, O, S): application to substituent effects, gas phase acidities and redox potentials. *J. Phys. Chem. A* **1999**, *103*, 1653–1661.
- (59) Wright, J. S.; Johnson, E. R.; DiLabio, G. A. Predicting the activity of phenolic antioxidants. *J. Am. Chem. Soc.* **2001**, *123*, 1173–1183.
- (60) Shadnia, H.; Wright, J. S. Understanding the toxicity of phenols: using quantitative structure–activity relationship and enthalpy changes to discriminate between possible mechanisms. *Chem. Res. Toxicol.* **2008**, *21*, 1197–1204.
- (61) Wright, J. S.; Shadnia, H. Computational modeling of substituent effects on phenol toxicity. *Chem. Res. Toxicol.* **2008**, *21*, 1426–1431.
- (62) Morgan, P.; Maggs, J. L.; Bulman-Page, P. C.; Hussain, F.; Park, B. K. The metabolism of 2- and 4-fluoro-17 β -estradiol in the rat and its implications for estrogen carcinogenesis. *Biochem. Pharmacol.* **1992**, *43*, 985–994.
- (63) Liehr, J. G. 2-Fluoroestradiol. Separation of estrogenicity from carcinogenicity. *Mol. Pharmacol.* **1983**, *23*, 278–281.
- (64) Siraki, A. G.; Chevaldina, T.; Moridani, M. Y.; O'Brien, P. J. Quantitative structure–toxicity relationships by accelerated cytotoxicity mechanism screening. *Curr. Opin. Drug Discovery Dev.* **2004**, *7* (1), 118–125.
- (65) The PDB file for 1GWR.pdb can be downloaded from www.rcsb.org.
- (66) (a) Warnmark, A.; Treuter, E.; Gustafsson, J. A.; Hubbard, R. E.; Brzozowski, A. M.; Pike, A. C. W. Interaction of transcriptional intermediary factor 2 nuclear receptor box peptides with the coactivator binding site of estrogen receptor α . *J. Biol. Chem.* **2001**, *277*, 21862–21868. (b) Kuiper, G. G. J. M.; Lemmen, J. G.; Carlsson, B.; Corton, J. C.; Safe, S. H.; Van Der Saag, P. T.; Van Der Burg, B.; Gustafsson, J. A. Interaction of estrogenic chemicals and phytoestrogens with estrogen receptor β . *Endocrinology* **1998**, *139*, 4252–4263.
- (67) Brandt, M. E.; Vickery, L. E. Cooperativity and dimerization of recombinant human estrogen receptor hormone-binding domain. *J. Biol. Chem.* **1997**, *272*, 4843–4849.
- (68) Obourn, J. D.; Koszewski, N. J.; Notides, A. C. Hormone- and DNA-binding mechanisms of the recombinant human estrogen receptor. *Biochemistry* **1993**, *32*, 6229–6236.
- (69) Bourgoin-Voillard, S.; Gallo, D.; Laïos, I.; Cleeren, A.; El Bali, L.; Jacquot, Y.; Nonclercq, D.; Laurent, G.; Tabet, J. C.; Leclercq, G. Capacity of type I and II ligands to confer to estrogen receptor α an appropriate conformation for the recruitment of coactivators containing a LxxLL motif—Relationship with the regulation of receptor level and ERE-dependent transcription in MCF-7 cells. *Biochem. Pharmacol.* **2010**, *79*, 746–757.
- (70) Moridani, M. Y.; Siraki, A.; O'Brien, P. J. Quantitative structure toxicity relationships for phenols in isolated rat hepatocytes. *Chem.-Biol. Interact.* **2003**, *145* (2), 213–223.
- (71) Ward, D. E.; Jheengut, V. Proline-catalyzed asymmetric aldol reactions of tetrahydro-4H-thiopyran-4-one with aldehydes. *Tetrahedron Lett.* **2004**, *45*, 8347–8350.
- (72) Aman, A.; Wright, J. S.; Durst, T. Unpublished results.